AD-A033 233 WEIDLINGER ASSOCIATES NEW YORK F/G 8/11
MATERIAL MODELING BASED ON CIST TEST AND LABORATORY DATA.(U)
MAR 76 I S SANDLER DNA001-75-C-0239
UNCLASSIFIED DNA-3970F NL

1 OF 1
AD
A033233

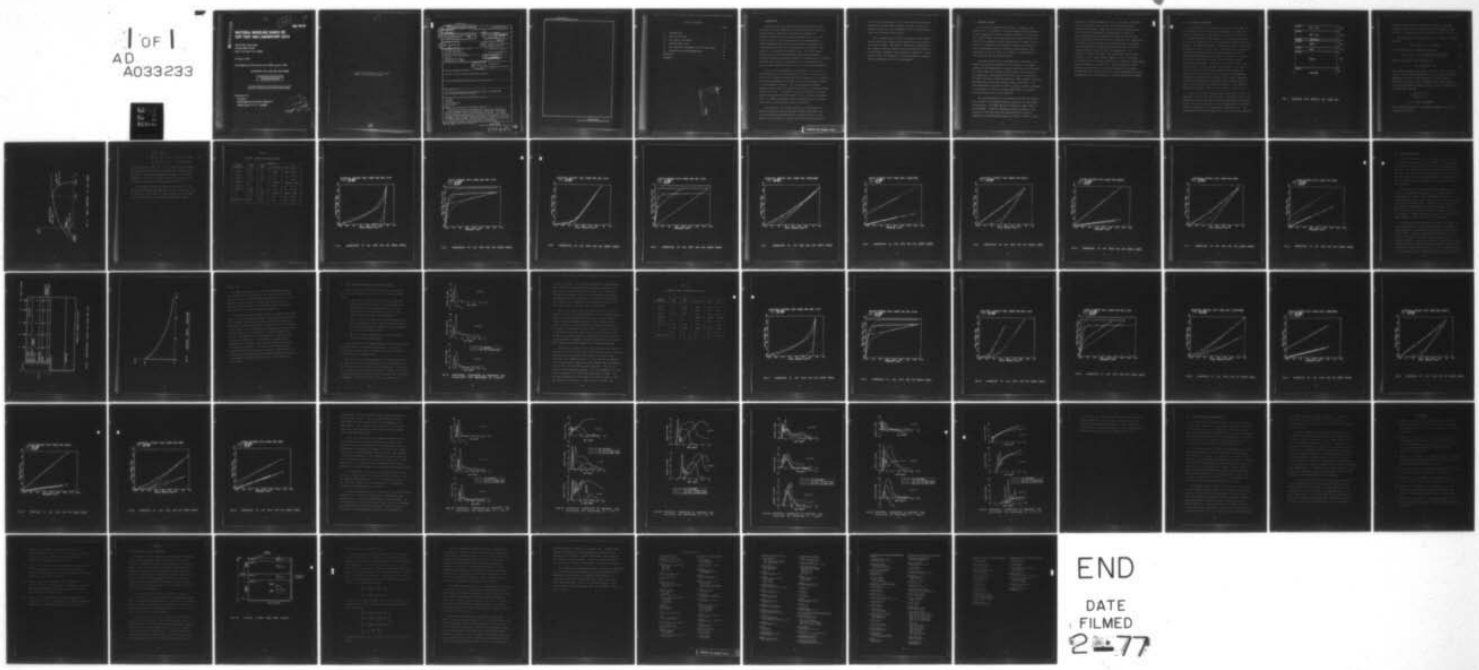

END

DATE
FILMED
2-77

DNA 3970F

MATERIAL MODELING BASED ON CIST TEST AND LABORATORY DATA

Weidlinger Associates
110 East 59th Street
New York, New York 10022

31 March 1976

Final Report for Period February 1975—January 1976

CONTRACT No. DNA 001-75-C-0239

APPROVED FOR PUBLIC RELEASE;
DISTRIBUTION UNLIMITED.

THIS WORK SPONSORED BY THE DEFENSE NUCLEAR AGENCY
UNDER RDT&E RMSS CODE B344075464 Y99QAXSB04789 H2590D.

Prepared for
Director
DEFENSE NUCLEAR AGENCY
Washington, D. C. 20305

Destroy this report when it is no longer needed. Do not return to sender.

UNCLASSIFIED

SECURITY CLASSIFICATION OF THIS PAGE (When Data Entered)

REPORT DOCUMENTATION PAGE

READ INSTRUCTIONS BEFORE COMPLETING FORM

1. REPORT NUMBER: DNA 3970F	2. GOVT ACCESSION NO.
3. RECIPIENT'S CATALOG NUMBER	
4. TITLE (and Subtitle): MATERIAL MODELING BASED ON CIST TEST AND LABORATORY DATA	5. TYPE OF REPORT & PERIOD COVERED: Final Report for Period Feb 75—Jan 76
6. PERFORMING ORG. REPORT NUMBER	
7. AUTHOR(s): Dr. I.S. Sandler	8. CONTRACT OR GRANT NUMBER(s): DNA 001-75-C-0239
9. PERFORMING ORGANIZATION NAME AND ADDRESS: Weidlinger Associates, 110 East 59th Street, New York, New York 10022	10. PROGRAM ELEMENT, PROJECT, TASK AREA & WORK UNIT NUMBERS: Subtask Y99QAXSB047-89
11. CONTROLLING OFFICE NAME AND ADDRESS: Director, Defense Nuclear Agency, Washington, D.C. 20305	12. REPORT DATE: 31 March 1976
	13. NUMBER OF PAGES: 64
14. MONITORING AGENCY NAME & ADDRESS (if different from Controlling Office): 59 p.	15. SECURITY CLASS (of this report): UNCLASSIFIED
	15a. DECLASSIFICATION/DOWNGRADING SCHEDULE

16. DISTRIBUTION STATEMENT (of this Report)

Approved for public release; distribution unlimited.

17. DISTRIBUTION STATEMENT (of the abstract entered in Block 20, if different from Report)

18. SUPPLEMENTARY NOTES

This work sponsored by the Defense Nuclear Agency under RDT&E RMSS Code B344075464 Y99QAXSB04789 H2590D.

19. KEY WORDS (Continue on reverse side if necessary and identify by block number)

Cap Model
CIST Test
In Situ Properties
Ground Shock

20. ABSTRACT (Continue on reverse side if necessary and identify by block number)

An iterative procedure is presented for constructing mathematical constitutive models for use in ground shock calculations. The procedure uses both laboratory and in situ (CIST) data for modeling. An original cap model based on laboratory data is adjusted in such a way as to achieve agreement between CIST measurements and a numerical computation of the CIST experiment using the model. The final model which results can then be used to represent the site for other ground shock calculations.

DD FORM 1 JAN 73 1473 EDITION OF 1 NOV 65 IS OBSOLETE

UNCLASSIFIED

SECURITY CLASSIFICATION OF THIS PAGE (When Data Entered)

373050

TABLE OF CONTENTS

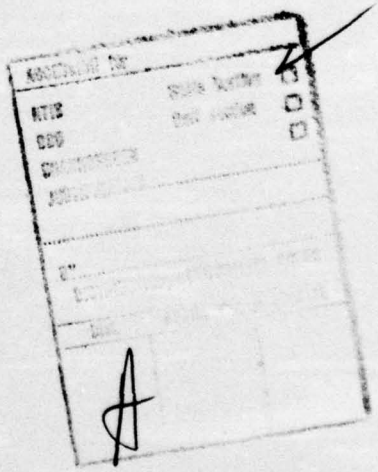

I INTRODUCTION

During the past few years, it has become apparent that problems of wave propagation in the earth cannot be adequately studied without appropriate information regarding the mechanical behavior of the in situ material, Refs. [1], [2], and [3]. Any or all of the practices of coring, sampling, sample preparation and testing may introduce substantial uncertainties and errors into any laboratory assessment of the behavior of a particular geological site. For this reason, various in situ testing procedures have been developed to directly determine the ground response to various types of loading. This data can be used in conjunction with laboratory data to obtain a more complete picture of the in situ material behavior.

One of the more promising of the dynamic in situ tests is the Cylindrical In Situ Test (CIST), Ref. [4]. In such a test, a vertical cylindrical cavity two feet in diameter is explosively loaded (and subsequently unloaded as the cavity pressure decays) in an axisymmetric fashion. The cavity generally extends through several layers of geological materials to depths ranging from 30 to 75 feet. A number of vertical boreholes at various ranges and azimuths from the central cavity contain instrumentation at a number of depths to measure ground motion in various directions in the different layers of material.

The purpose of the present study is to investigate the means by which the results obtained in CIST experiments can be utilized in the construction of a material model to represent in situ behavior. Because the CIST configuration does

not exercise the material in all stress and/or strain paths expected in a ground shock problem, the use of data from laboratory tests is also incorporated into the modeling procedure as described in this report.

The cap model, Refs. [5]-[7], was used for this study because many recent ground shock computations have utilized this type of model. The model is capable of representing a wide range of material behavior while satisfying conditions of existence, uniqueness and stability of solution. In the present study, the capability of the cap model to represent material behavior in CIST is investigated.

II OUTLINE OF STUDY

The procedure employed in this study is based on the premise that, if possible, the material model should represent as many important features of material behavior as is practical. Specifically, one should select the manner in which the CIST test is employed for the construction of a model in such a way as to minimize the differences between the behavior of the resulting model and the laboratory based property data (provided, of course, there is no inherent inconsistency between the CIST and laboratory results).

The most natural way to accomplish this objective is to define the qualitative behavior of the material in a number loading and unloading paths. Because materials can be subjected to a wide range of controlled stress and/or strain paths in the laboratory, the laboratory data will lead to a selection of model functional forms and parameters which properly represent the variations in material behavior under these paths. The CIST measurements can then be used to adjust the model parameters (if possible) to arrive at a final model which is in quantitative agreement with in situ behavior.

The starting point for the present study involves fitting the cap model to available laboratory data for the site under consideration - the HARD PAN site in Kansas at which CIST 12 was performed. Using the laboratory based cap model, a calculation of the CIST event was performed and the results compared to the measurements made during CIST. Based on these

comparisons, several changes were made in the model parameters and the calculations were rerun. An iterative procedure involving computation, comparison of results and measurements, and alteration of the model, was undertaken in order to reduce the discrepancies between experiment and calculation until satisfactory CIST results were obtained in the computation. As expected it was necessary to relinquish some of the quantitative agreement of the model and laboratory data in order to achieve improved results in the CIST computation. The differences between the final CIST based model and the laboratory data are not unduly large, however, and are considered to be well within the usual uncertainties involved in representing material behavior at a real site. The CIST based cap model obtained in this study is currently being used to represent the HARD PAN site in free-field and structure-medium interaction problems for the Space and Missile Systems Organization (SAMSO).

III SITE PROFILE AND MODEL

The particular site chosen for this study is the HARD PAN site in Kansas at which CIST 12 was performed. The HARD PAN series of field tests is designed to investigate the response of a scaled Minuteman Launch Facility to explosively generated air blast and ground shock in an interbedded clay/shale/limestone geology. The HARD PAN geology is complex and varies significantly from point to point over the site. An idealized and simplified site profile based on Refs.[8]-[10] was chosen for the CIST calculations performed in this study in an attempt to "average" the material properties for each layer in which the CIST measurements were taken. There are two reasons to make such a simplification. First, the exact site profile is not known for each CIST guage hole; it varies somewhat with aziumth and range from the central CIST cavity. Second, two dimensional axisymmetric calculations of practical size cannot adequately represent that portion of the ground signal arising from such small scale variations in material properties. The idealized HARD PAN site profile chosen for this study is shown in Fig. 1.

A set of laboratory based data which describes the material behavior of each of the layers of Fig. 1 was taken from Ref. [8]. Although a more detailed set of material properties is included in Ref. [9], the use of such a set of properties for the present study is not warranted for the reasons described above. The laboratory based material behavior for each of the five materials

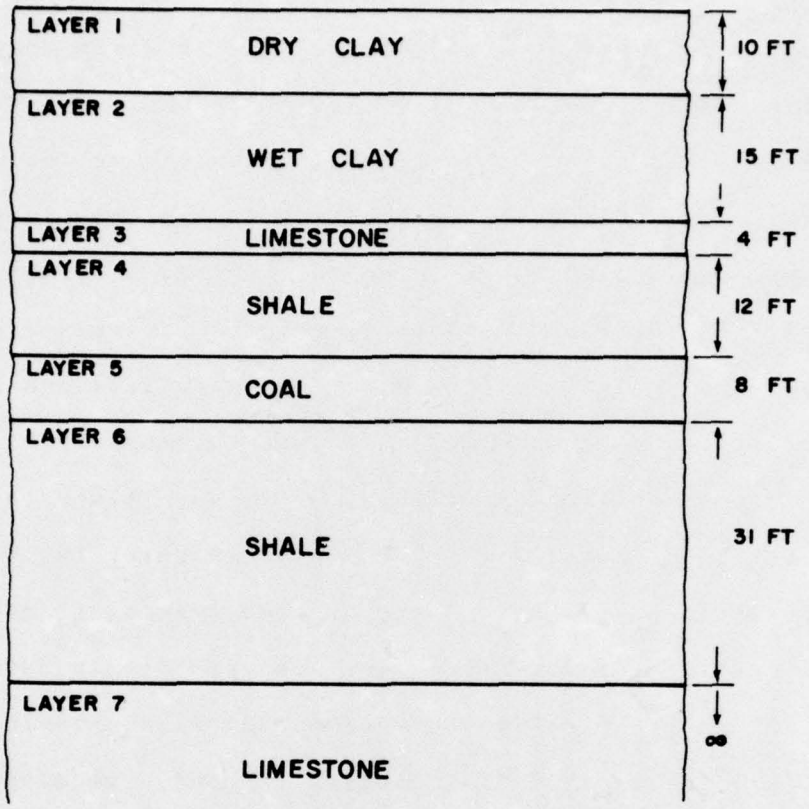

FIG. 1 IDEALIZED SITE PROFILE FOR HARD PAN

included in the current study was fit by means of an eight parameter version of the cap model, Ref. [5], modified, where required, to represent rocks as described in Refs. [6] and [7].

The model, which is depicted in Fig. 2, includes a failure envelope,

$$\sqrt{J_2'} = F_F(J_1) = A - C \exp(BJ_1) \tag{1}$$

an elliptical cap of constant eccentricity,

$$\sqrt{J_2'} = F_c(J_1,\kappa) = \frac{1}{R}\sqrt{[X(\kappa)-L(\kappa)]^2 - [J_1-L(\kappa)]^2} \tag{2}$$

which is governed by the hardening rule

$$\bar{\varepsilon}_v^p = W[\exp(DX) - 1] \tag{3}$$

and constant bulk and shear moduli, K and G, within the yield surface. In the above equations A, B, C, R, W and D are model parameters, J_1 is the first invariant of stress (tension positive), J_2' is the second invariant of the stress deviators, κ is the cap hardening parameter and X and L are functions of κ through the relations

$$L = \begin{cases} \kappa \text{ if } \kappa \leq 0 \\ 0 \text{ if } \kappa > 0 \end{cases} \tag{4}$$

$$X = \kappa - R[A - C \exp(B\kappa)]$$

The quantity $\bar{\varepsilon}_v^p$ depends on the plastic volumetric strain, ε_v^p, through the relations

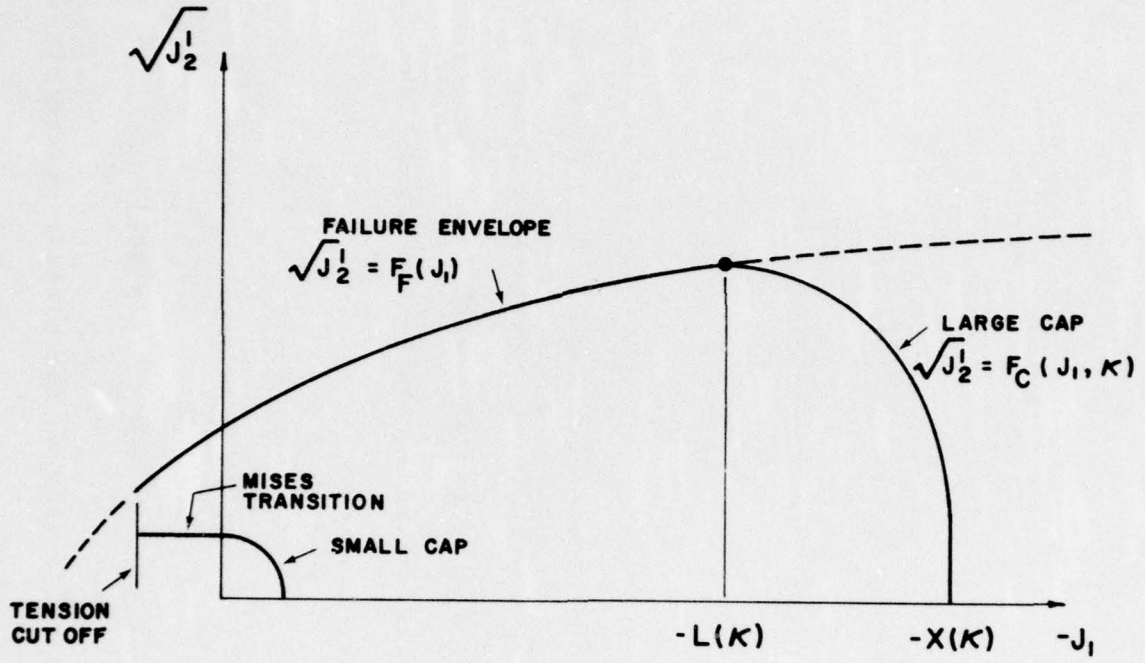

FIG. 2 YIELD SURFACES IN CAP MODEL

$$\dot{\varepsilon}_v^D = \begin{cases} \dot{\varepsilon}_v^p \text{ if } \dot{\varepsilon}_v^p \leq 0 \\ \dot{\varepsilon}_v^p \text{ if } \dot{\varepsilon}_v^p > 0 \text{ and } \kappa < 0 \text{ for soils only} \\ 0 \text{ if } \dot{\varepsilon}_v^p > 0 \text{ for } \kappa \geq 0 \text{ or for rocks} \end{cases} \quad (5)$$

In this study the clays, i.e., the two upper layers in Fig.1, are considered to be soils. The material is assumed to be incapable of supporting hydrostatic tension - all stresses components are set to zero when hydrostatic tension occurs. The model is described in greater detail in Ref. [7].

The parameter values for which the cap model fits the laboratory based material behavior are listed in Table I, and the behavior of this model is shown in Figs. (3-12) together with the laboratory data to which the model was fitted.

TABLE I

CAP MODEL BASED ON LABORATORY DATA

MODEL PARAMETER	MATERIAL				
	DRY CLAY	WET CLAY	LIMESTONE	SHALE	COAL
K(ksi)	725.	725.	1600.	1160.	290.
G(ksi)	2.9	4.35	957.	247.	174.
A(ksi)	.0334	.016	58.	55.2	33.8
$B(ksi^{-1})$	0.	0.	.00966	.00966	.00966
C(ksi)	0.	0.	57.1	55.1	33.4
$D(ksi^{-1})$	.483	3.45	.69	.11	.586
W	.054	.0021	.00025	.0029	.002
R	2.3	2.5	3.5	5.0	3.8
Density (p.c.f.)	124.	128.	167.	155.	84.9

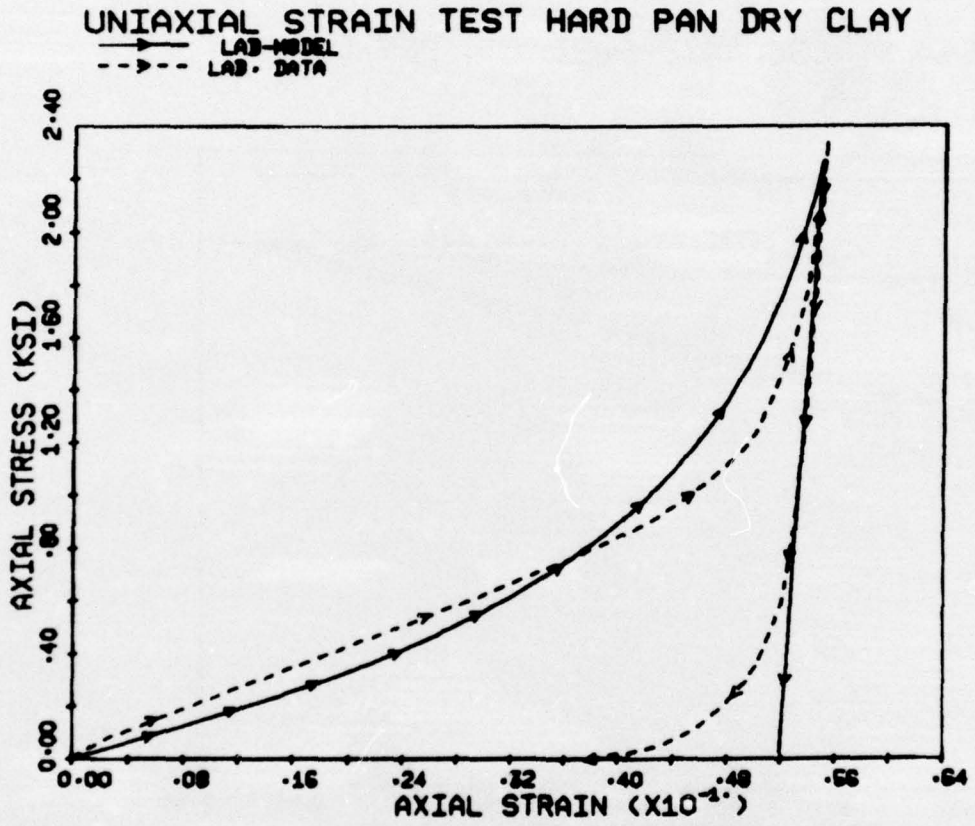

FIG. 3 COMPARISON OF LAB DATA AND LAB BASED MODEL

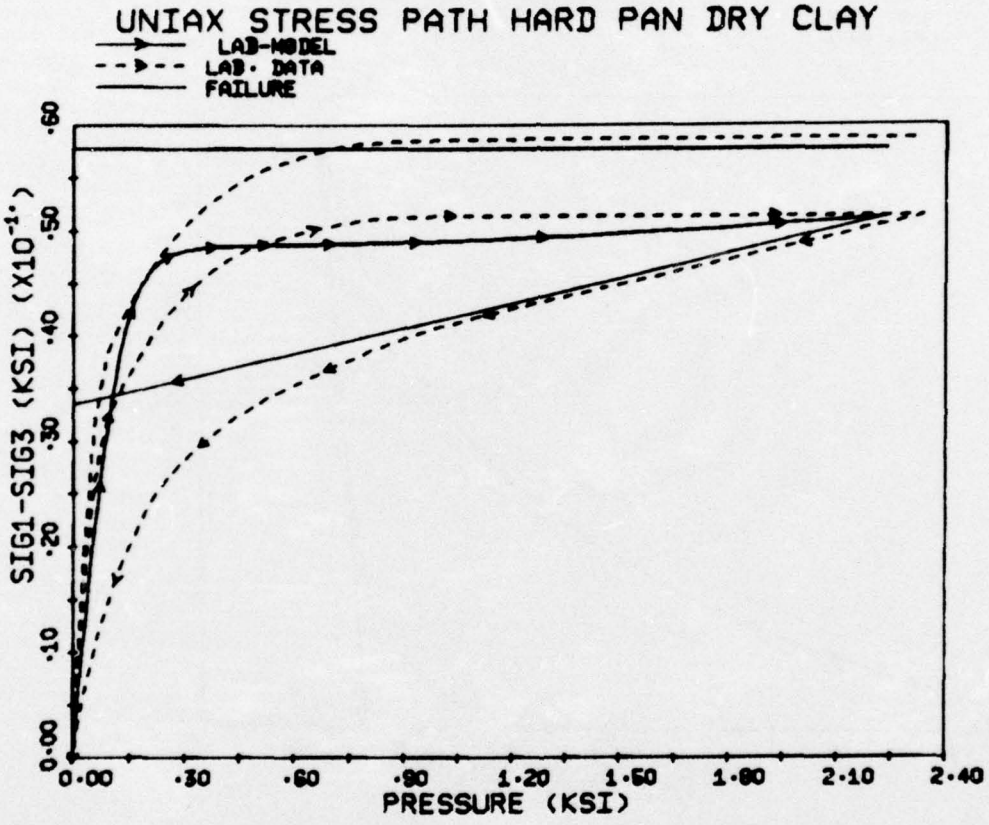

FIG. 4 COMPARISON OF LAB DATA AND LAB BASED MODEL

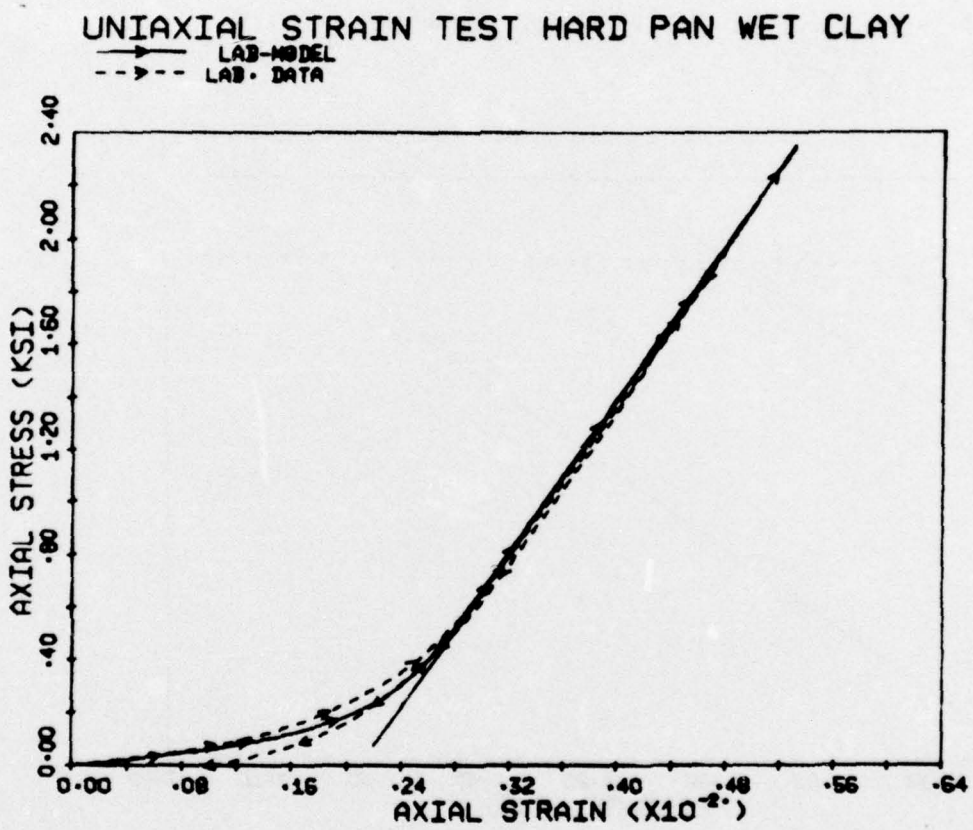

FIG.5 COMPARISON OF LAB DATA AND LAB BASED MODEL

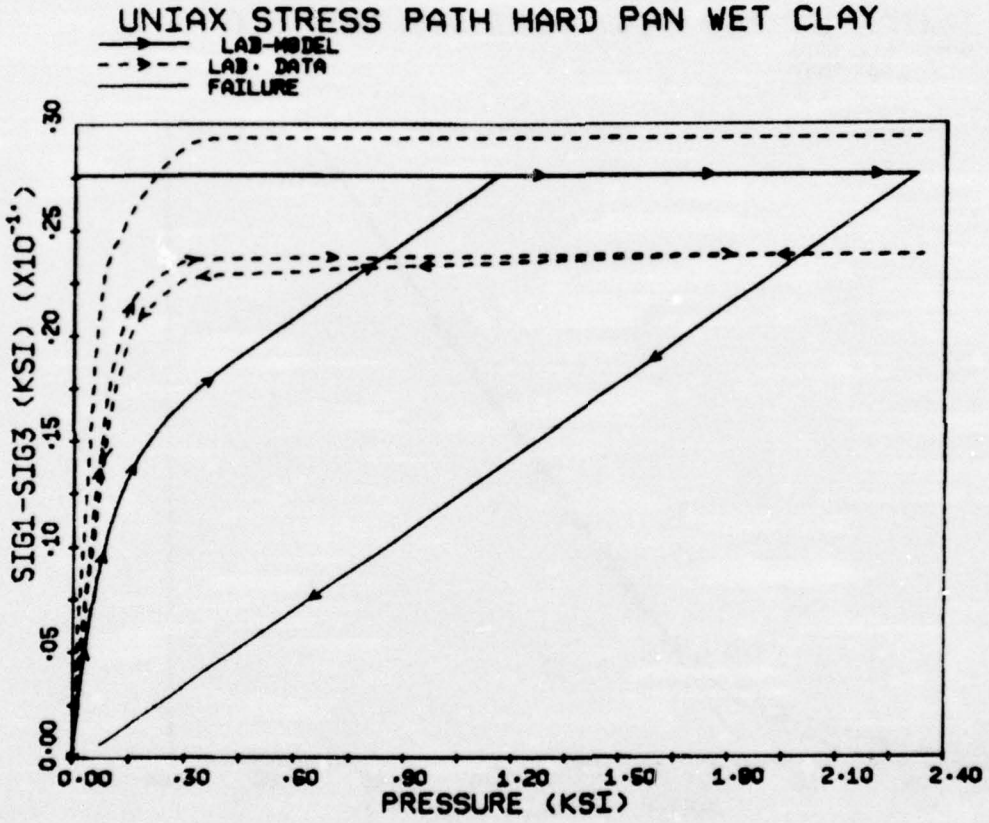

FIG.6 COMPARISON OF LAB DATA AND LAB BASED MODEL

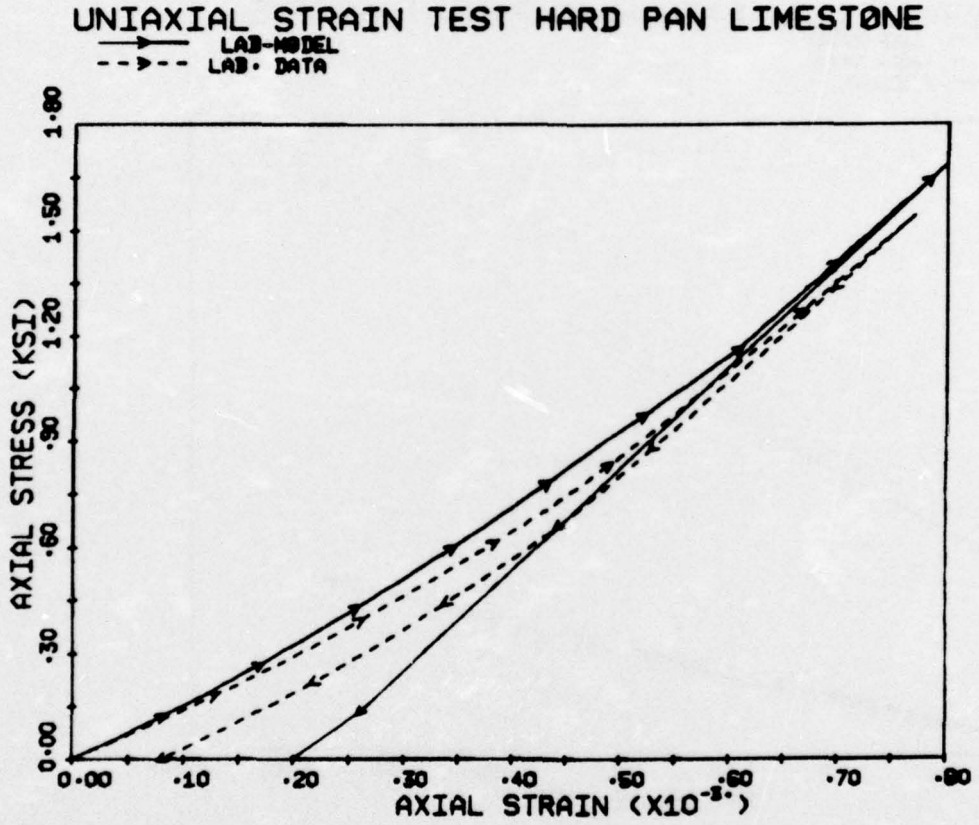

FIG.7 COMPARISON OF LAB DATA AND LAB BASED MODEL

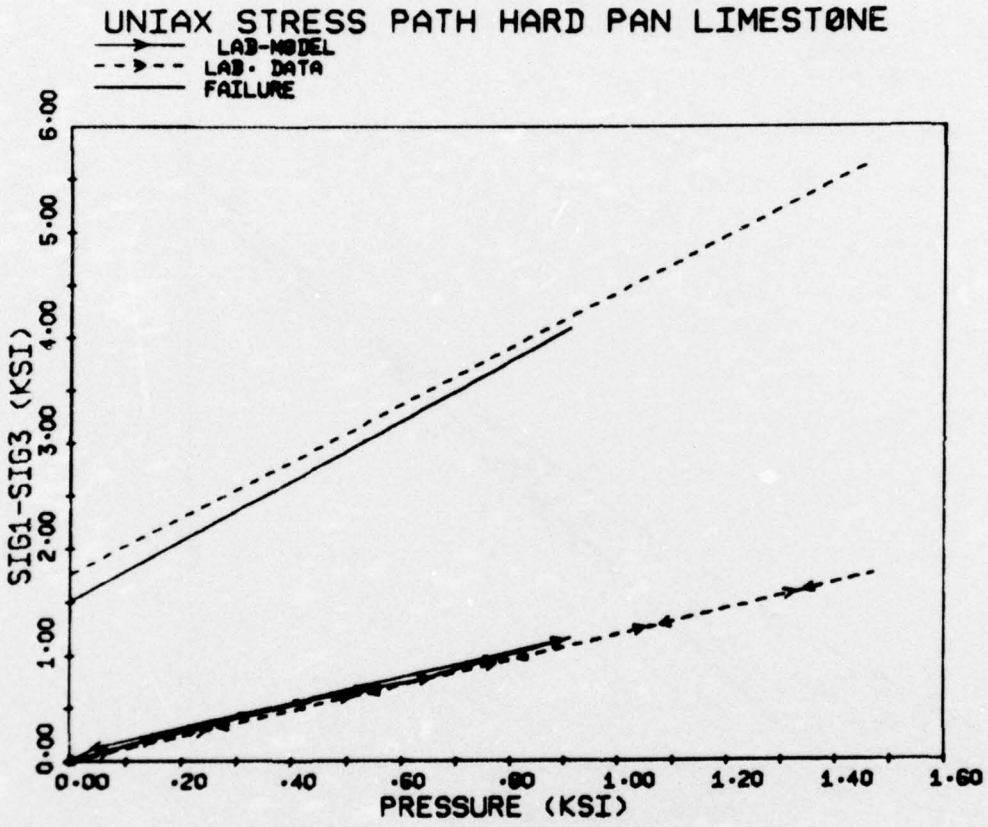

FIG. 8 COMPARISON OF LAB DATA AND LAB BASED MODEL

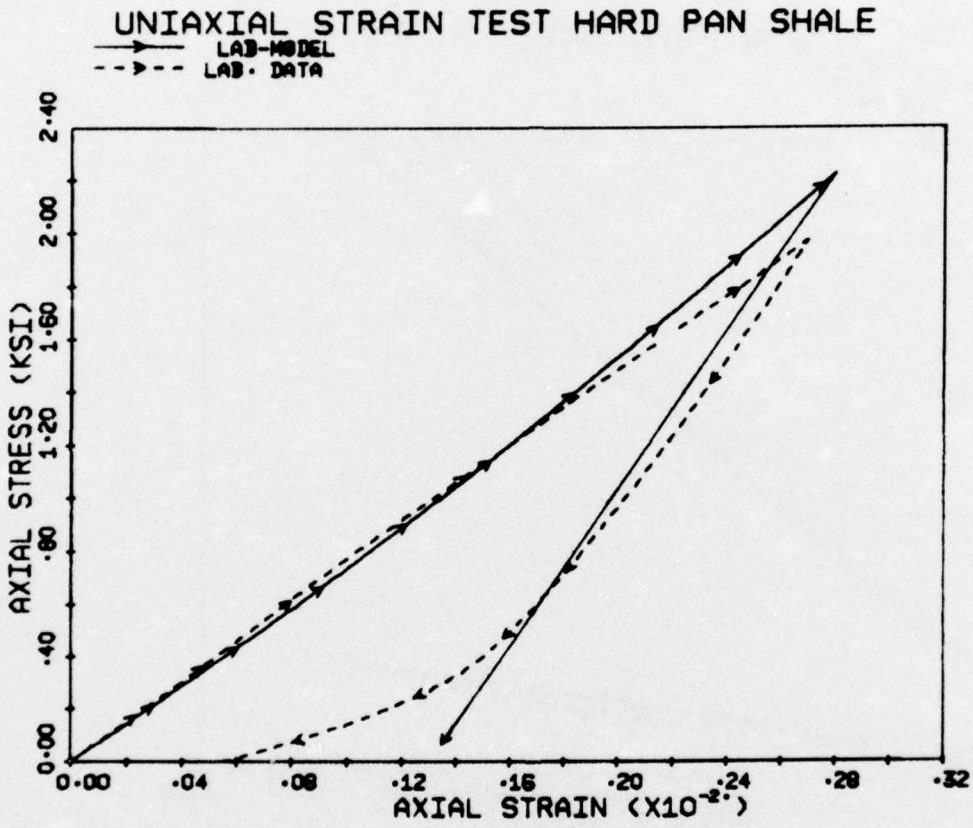

FIG. 9 COMPARISON OF LAB DATA AND LAB BASED MODEL

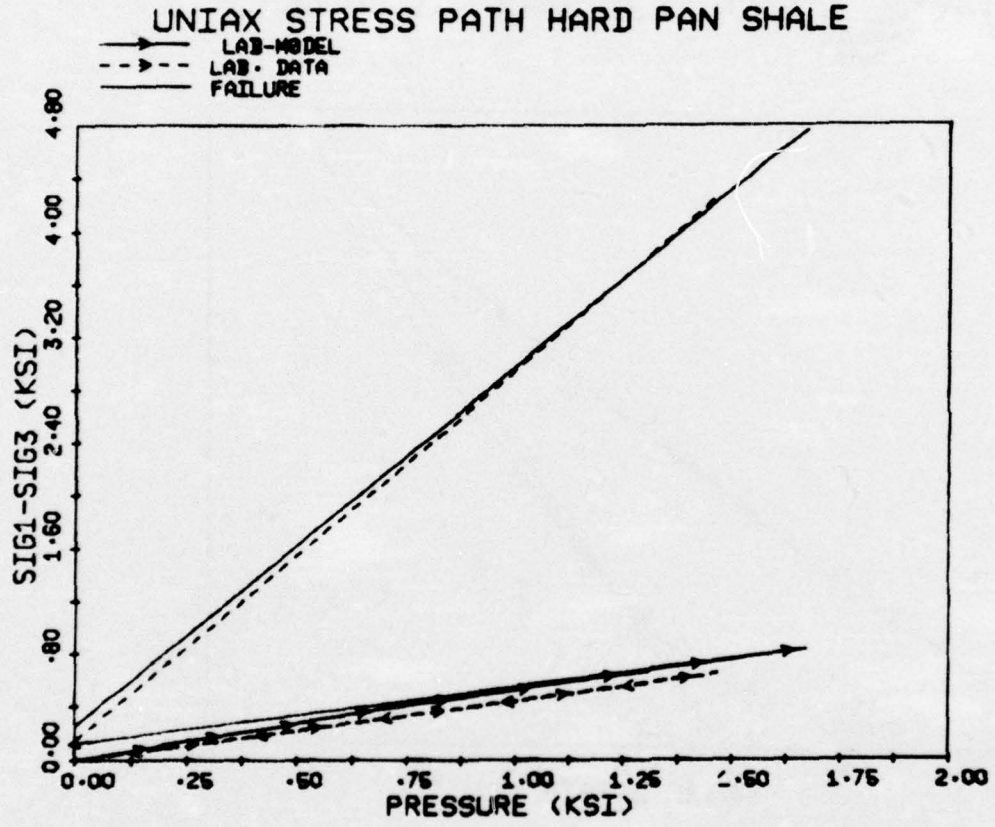

FIG. 10 COMPARISON OF LAB DATA AND LAB BASED MODEL

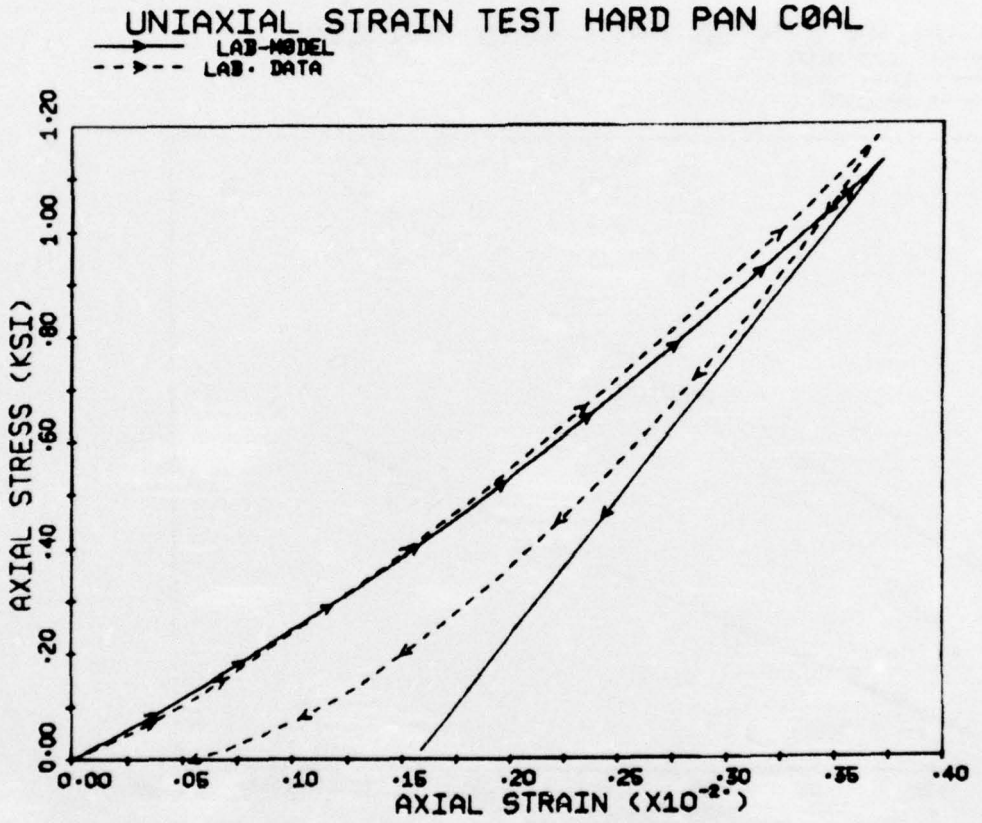

FIG. 11 COMPARISON OF LAB DATA AND LAB BASED MODEL

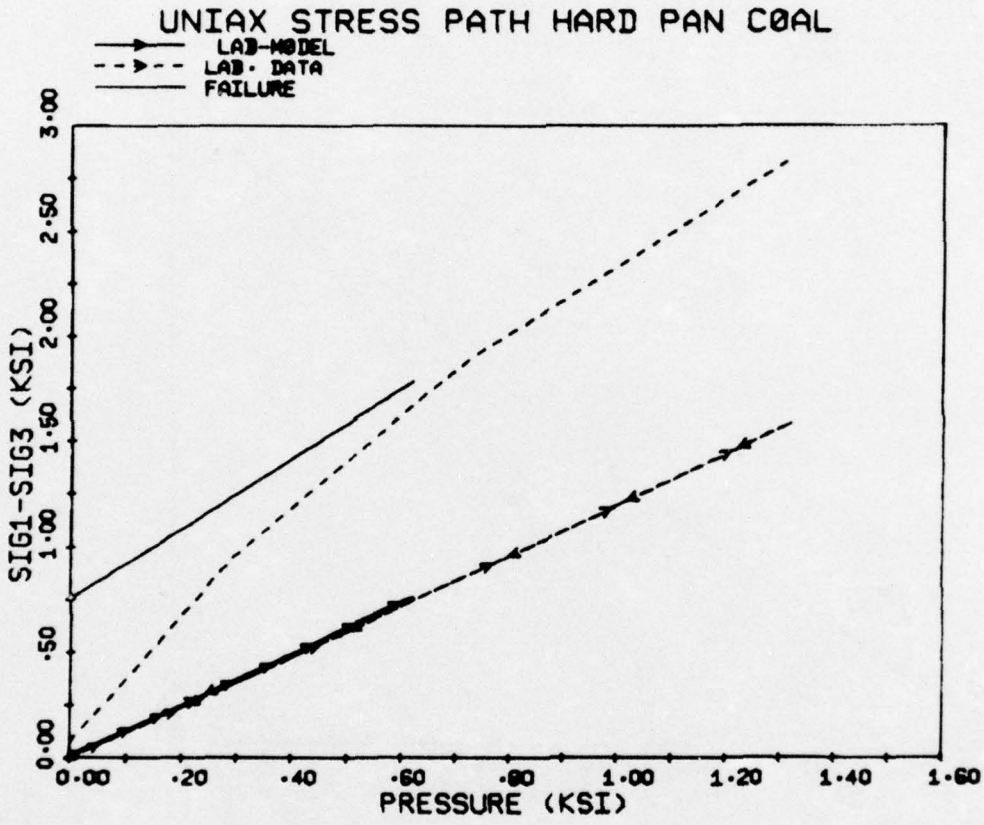

FIG. 12 COMPARISON OF LAB DATA AND LAB BASED MODEL

IV COMPUTATIONAL SETUP

The model described in the preceeding section was used to perform a calculation of the CIST Event. For this purpose the LAYER code, which is briefly described in the Appendix, was used. The computational grid layout is shown in Fig. (13). The time step for the calculation was 0.08 ms and the calculation was carried to a time of about 10 ms. The computation required approximately six minutes of central processor time on a CDC 6600.

The proper input loading for the CIST computation is a matter of considerable uncertainty. No reliable pressure measurement was obtained for the HARD PAN CIST test and considerable variation in the cavity pressure loadings has been observed in other CIST tests. Therefore it was decided that the nominal or idealized cavity pressure loading shown in Fig. 14 would be used unless it was later found to be incorrect or inadequate. During the present study no alteration of the input loading of Fig. 14 was found to be required.

Several checks were performed to validate the LAYER code setup to handle CIST. One and two dimensional axisymmetric calculations were performed with the bilinear material model of Ref. [11]. In these calculations variations were made in the grid size and the procedure used to apply the cavity pressure boundary condition to the grid. The results of these computations were compared to results obtained by means of the characteristic-based code of Ref. [11]. The agreement between the characteristic code and LAYER was quite good, as reported

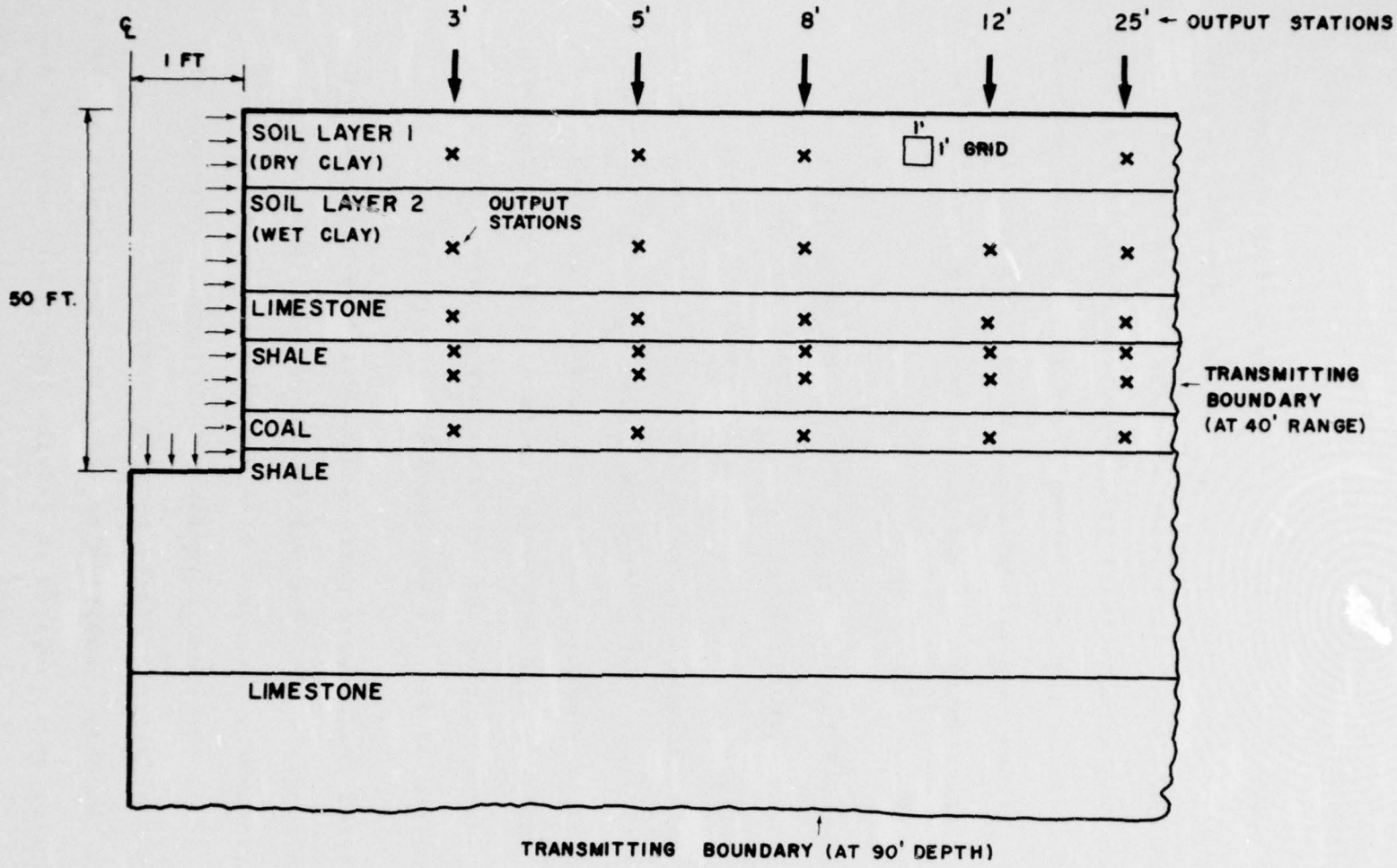

FIG. 13 COMPUTATIONAL LAYOUT FOR HARD PAN CIST

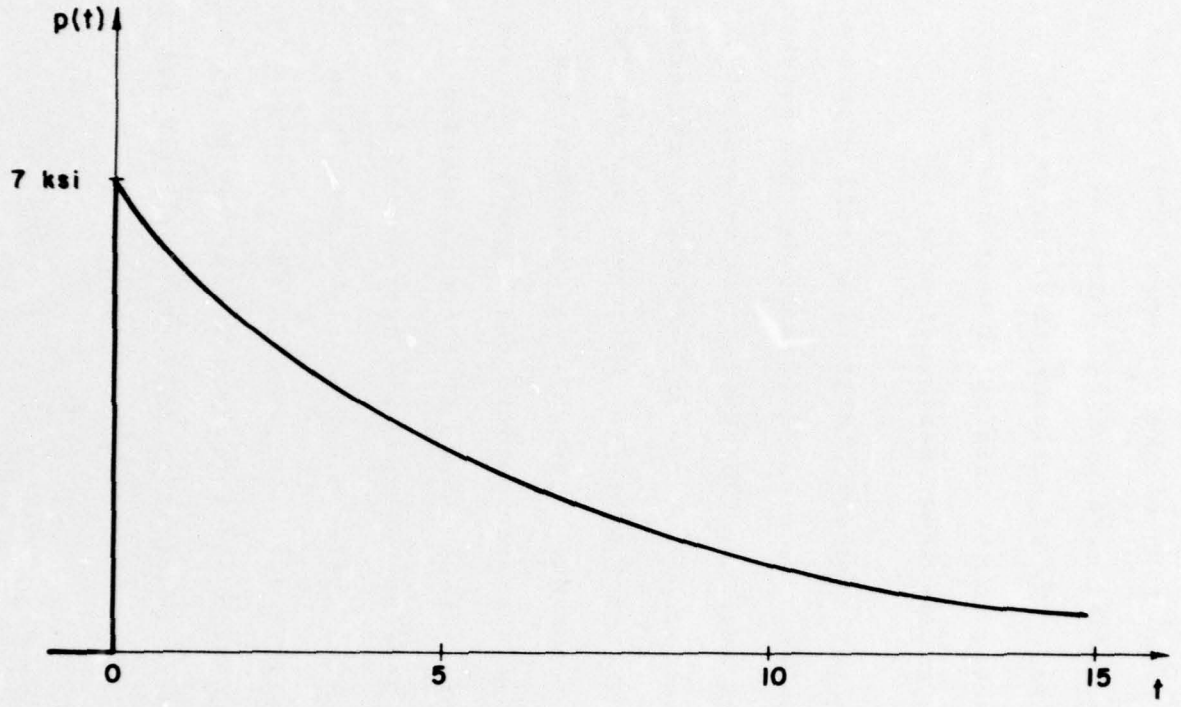

FIG. 14 APPLIED CAVITY PRESSURE

in Ref. [11].

An additional check on the effect of grid size was made by rerunning the early portion of the cap model CIST calculation with a 1/2 foot radial mesh spacing instead of the 1 foot spacing originally used. No significant differences were observed in the results, so the original 1 foot square mesh was retained for the entire study performed here.

As indicated in the Appendix, LAYER is a small displacement code, i.e., the assumption is made in this study that convection and transport effects near the CIST cavity can be neglected. Furthermore, the small air blast loading effects on the ground surface away from the cavity are also neglected, and the applied pressure, Fig. 14, is assumed to be uniform throughout the cavity. The agreement obtained between the computations and the measured CIST data - to be shown in the next section - indicates that the above assumptions are appropriate as well as extremely convenient. This is important because these assumptions drastically reduce the computer time required to perform a CIST computation and therefore enable one to perform the iteration procedure required in this study quickly and efficiently.

V THE ITERATION PROCEDURE AND CIST BASED MODEL

The iteration procedure used in this study to develop the final CIST based model consists of the following three steps:

1. Compare the results of the CIST calculations with measured CIST ground response, noting similarities and differences in the waveforms as well as the sensitivity of various waveform features to model changes made in previous CIST calculations.

2. Based on the above comparisons, determine physically acceptable model parameter changes which are likely to reduce the discrepancies between the CIST calculations and the CIST experimental data.

3. Make the required revisions in the material model and recalculate the CIST event.

These three steps are repeated until either a) satisfactory agreement between calculation and experiment is obtained, or b) inability of the model to represent the material behavior in the CIST event is demonstrated.

The iterative procedure employed in this study begins with the comparison of the CIST measurements and the results of the CIST calculation performed with the lab based model. A typical set of waveforms used for this comparison is shown in Fig. (15), in which the horizontal particle velocity versus time is plotted at ranges of 3 feet, 5 feet and 8 feet at a depth of 45 ft.

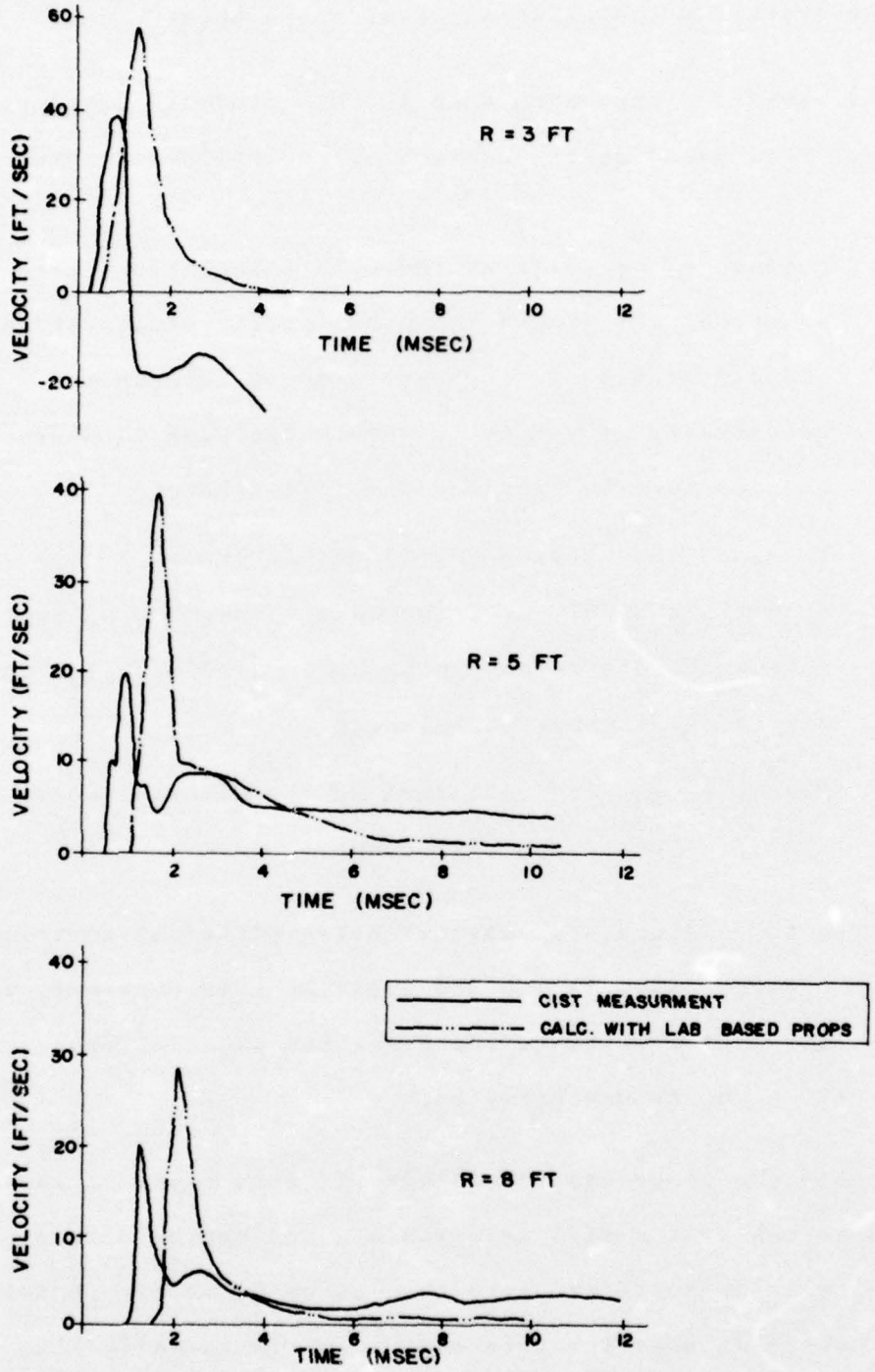

FIG. 15 HORIZONTAL COMPARISON OF MEASURED AND CALCULATED CIST WAVEFORMS AT Z = 45 FT.

(in the coal layer). The computed waveforms are qualitatively quite similar to the measured CIST waveforms, especially if one allows for baseline shift corrections to the CIST data. The major discrepancies between the calculated and measured waveforms occur in the magnitude of the peak velocity, which is too high in the computations, and the arrival time of the wave front, which is too late in the computations.

These facts suggest that the behavior of the lab based model is too soft for initial loading (a stiffer loading modulus tends to reduce peak particle velocity at the same time as it increases wave propagation speed, thereby reducing arrival time). Therefore, a stiffer loading behavior was introduced by halving the parameter W in all layers. This has the effect of halving the volumetric hysteresis, or locking strain, and increases the loading moduli of the material while leaving the unloading moduli unchanged. The CIST computation was repeated, thus completing the first cycle of the iteration procedure.

Although the results of the second computation were much improved, it was clear that further improvement could be obtained by increasing the unloading wave speeds in the model (and, therefore, the parameters K and G). This was done and several iteration loops were completed in which quantitative variations of K, G and W in the various layers were made. This is, of course, a trial and error process. The last computation of the series resulted in the final CIST based material model. The material parameters for this model are listed in Table II and the behavior of the model is shown in Figs. (16-25). The

TABLE II

CAP MODEL BASED ON ITERATION WITH CIST

MODEL PARAMETER	DRY CLAY	WET CLAY	LIME TONE	SHALE	COAL
K(ksi)	725.	1020.	2390.	1160.	580.
G(ksi)	2.9	6.09	1440.	247.	348.
A(ksi)	.0334	.016	58.0	55.2	33.8
$B(ksi^{-1})$	0.	0.	.00966	.00966	.00966
C(ksi)	0.	0.	57.1	55.1	33.4
$D(ksi^{-1})$	.483	3.45	.69	.11	.586
W	.054	.0011	.00013	.0029	.001
R	2.3	2.5	3.5	5.0	3.8
Density(p.c.f.)	124.	128.	167.	155.	84.9

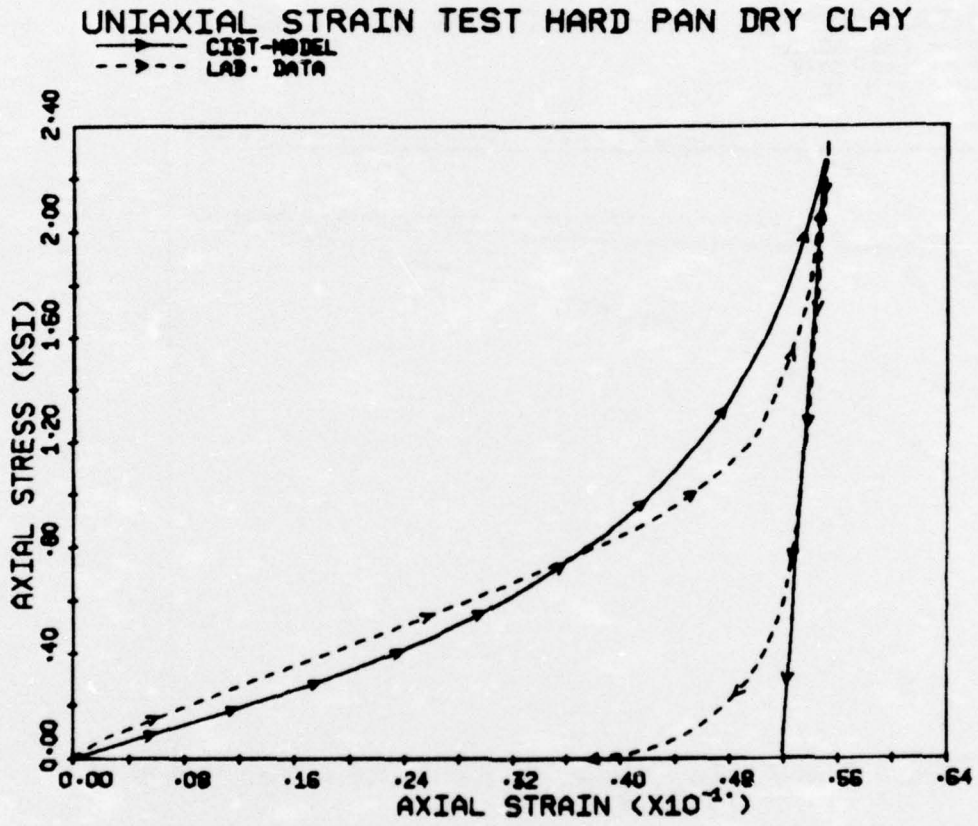

FIG. 16 COMPARISON OF LAB DATA AND CIST BASED MODEL

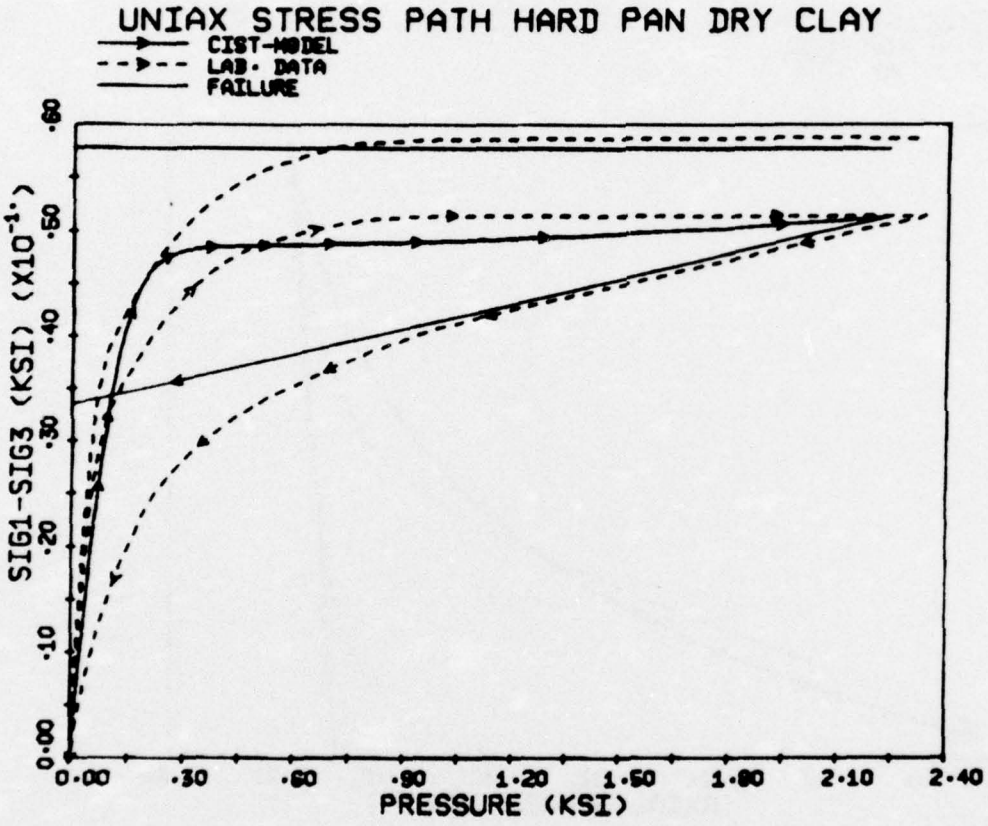

FIG. 17 COMPARISON OF LAB DATA AND CIST BASED MODEL

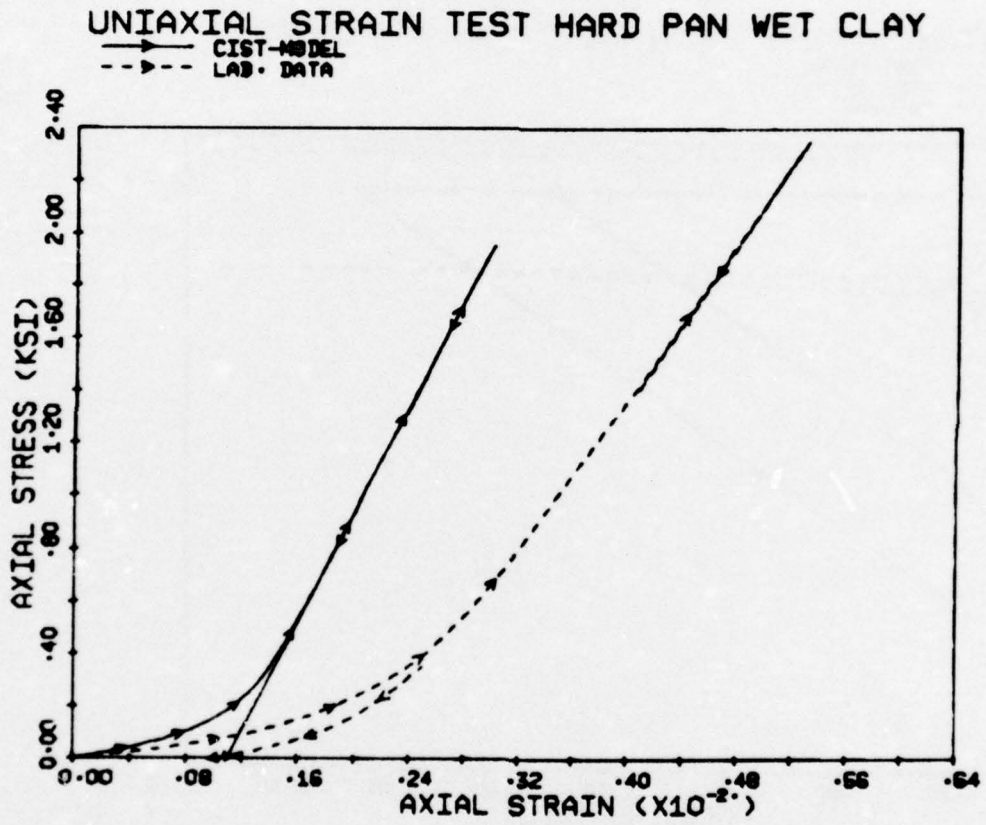

FIG. 18 COMPARISON OF LAB DATA AND CIST BASED MODEL

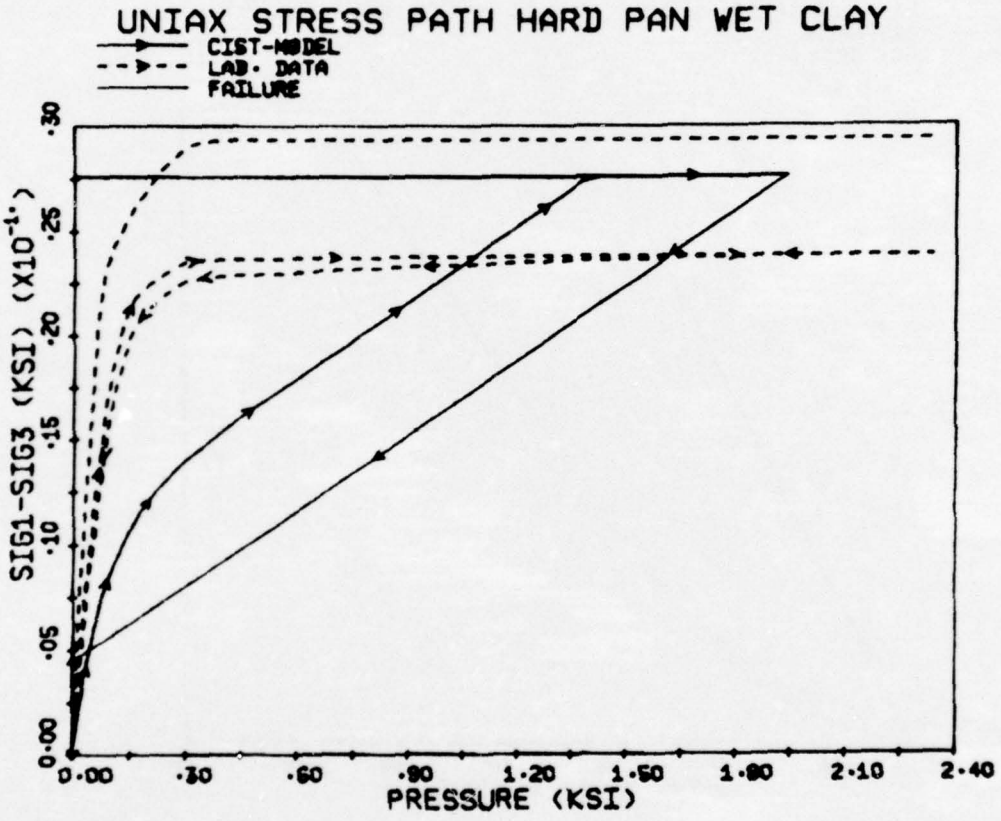

FIG. 19 COMPARISON OF LAB DATA AND CIST BASED MODEL

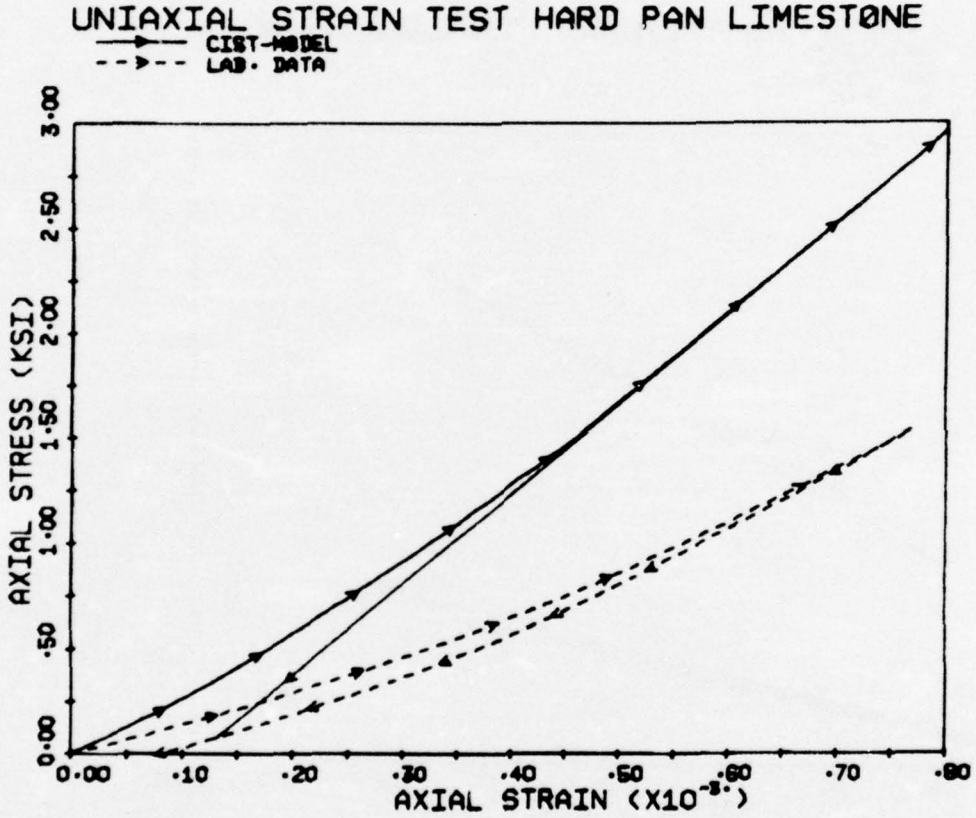

FIG. 20 COMPARISON OF LAB DATA AND CIST BASED MODEL

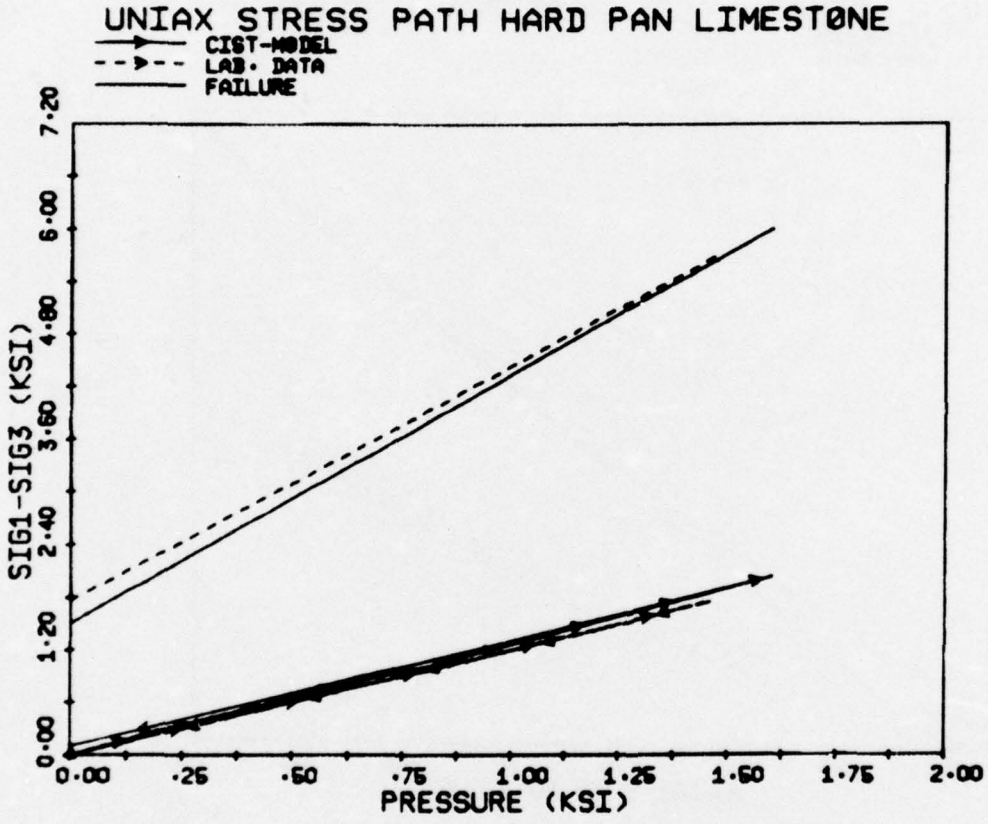

FIG. 21 COMPARISON OF LAB DATA AND CIST BASED MODEL

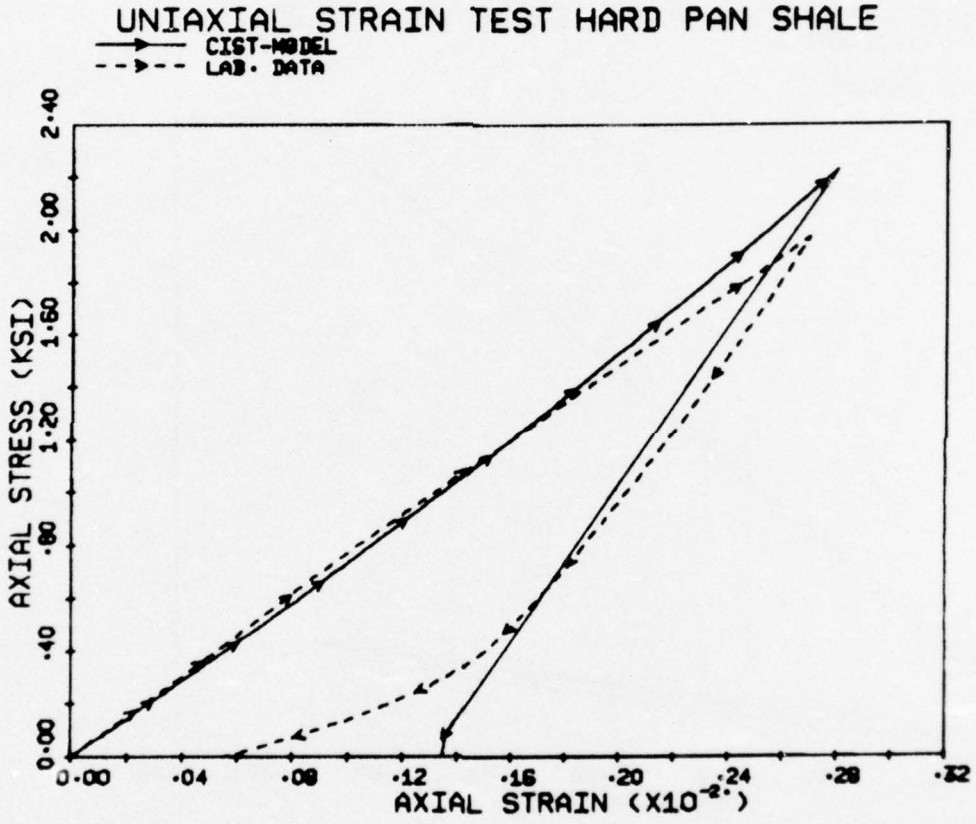

FIG. 22 COMPARISON OF LAB DATA AND CIST BASED MODEL

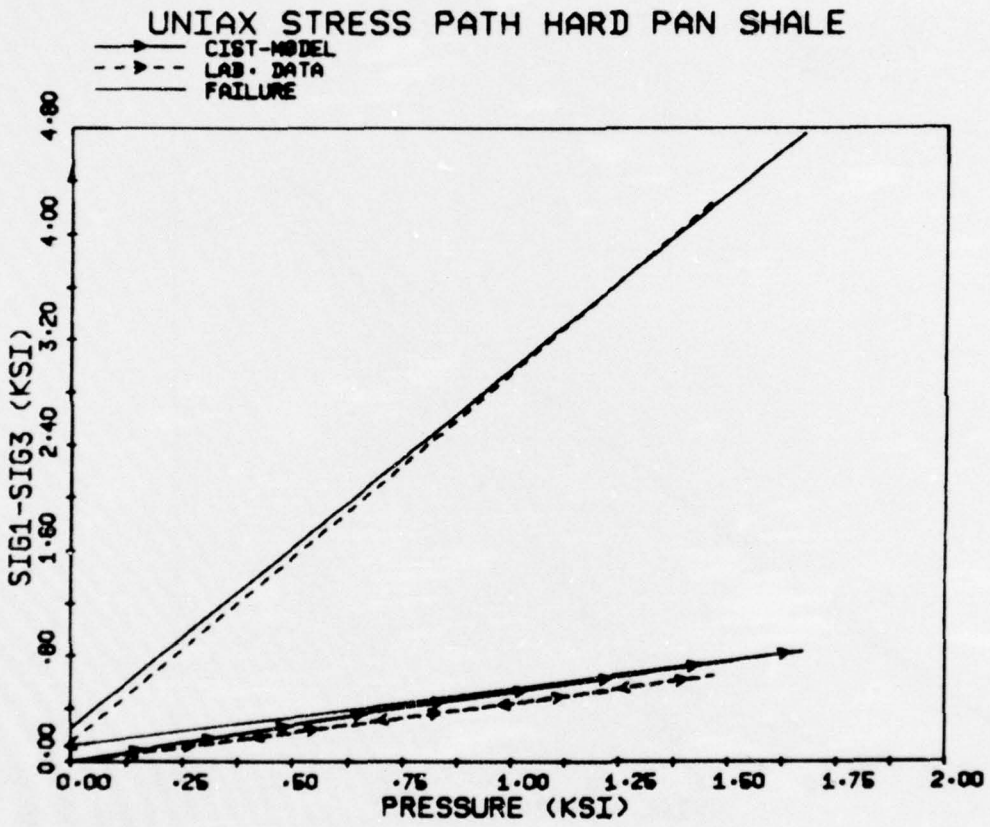

FIG. 23 COMPARISON OF LAB DATA AND CIST BASED MODEL

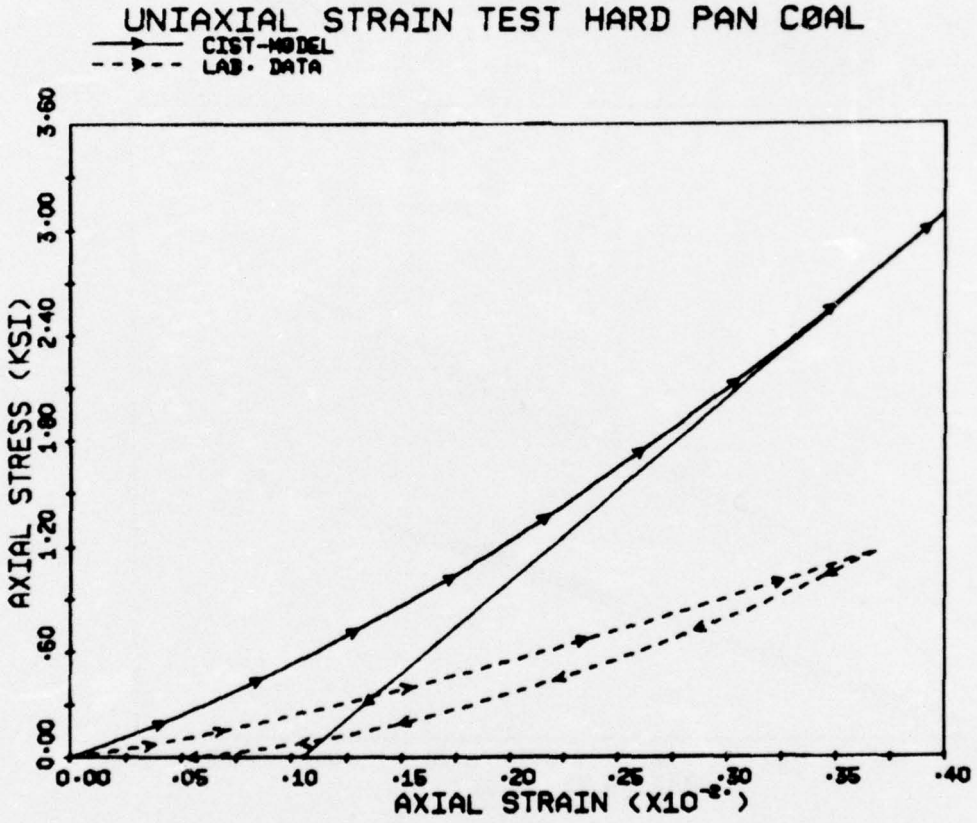

FIG. 24 COMPARISON OF LAB DATA AND CIST BASED MODEL

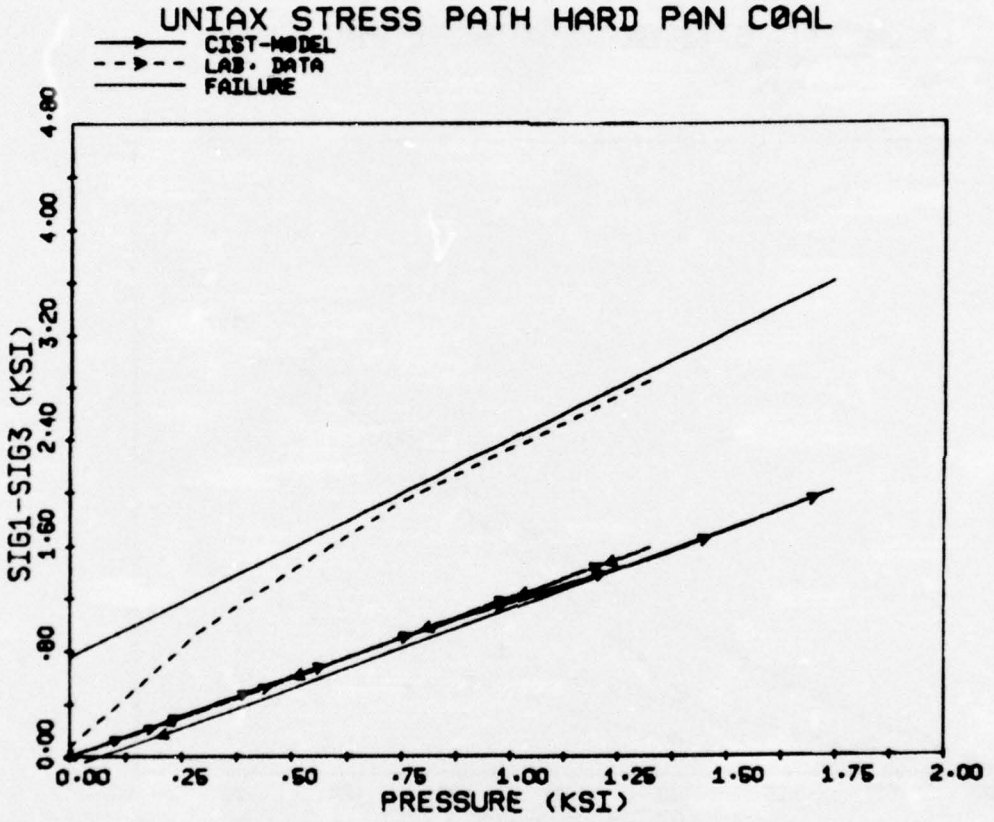

FIG.25 COMPARISON OF LAB DATA AND CIST BASED MODEL

computational results obtained with this CIST based model are shown in Figs. (26-31). They are labeled "CALC. WITH CIST BASED PROPS" and are compared with the correspopding CIST measurements. For convenience the results of the first CIST computation are also shown in these figures and are lableed "CALC. WITH LAB BASED PROPS".

Figure (26-31) show that the agreement between the CIST measurements and the final CIST computation is good. The computed magnitudes and waveforms of the horizontal velocity time-histories throughout the region of the CIST event compare well with the overall behavior measured in CIST. The agreement of the CIST measurements to the computational results obtained with the LAB based model is of course not as good, but is still substantial; it is possible that the LAB based model for the HARD PAN site would be adequate for many ground shock applications.

It is important to note that the CIST based model behavior as shown in Figs. (16-25) is not overwhelmingly different from the original laboratory data. It is reassuring that, at least for this site, a model has been obtained that can adequately represent both laboratory and in situ data.

It should be pointed out that, although all of the CIST results presented here involve horizontal motions, measurements and computations of vertical ground motions are also available. As one might expect, however, these do not agree well at all because the vertical motions in CIST are extremely sensitive to non-uniformity in the layering and to material non-homogeneity

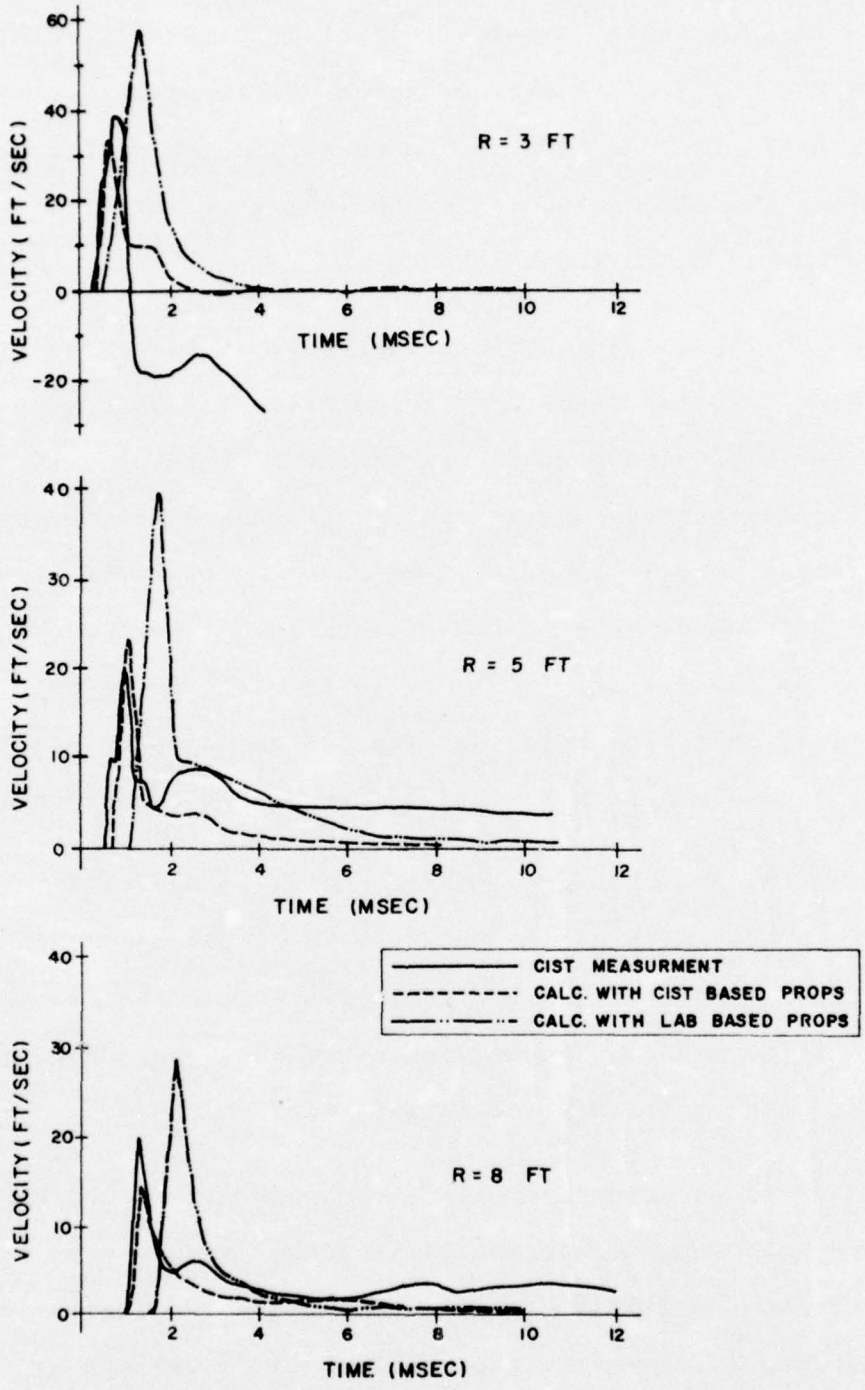

FIG. 26 HORIZONTAL - COMPARISON OF MEASURED AND CALCULATED CIST WAVEFORMS AT Z = 45 FT.

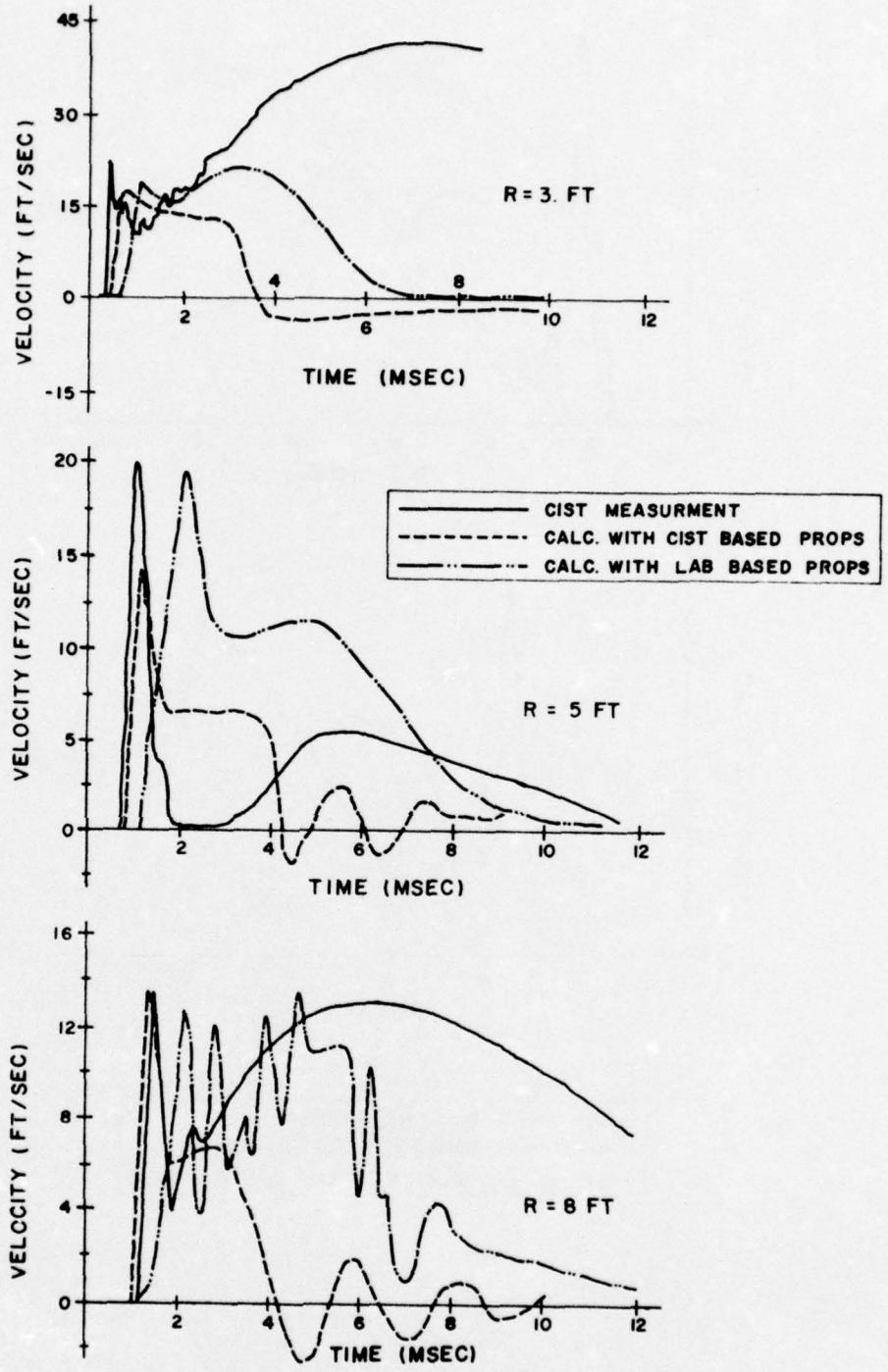

FIG. 27 HORIZONTAL- COMPARISON OF MEASURED AND CALCULATED CIST WAVEFORMS AT Z = 35 FT.

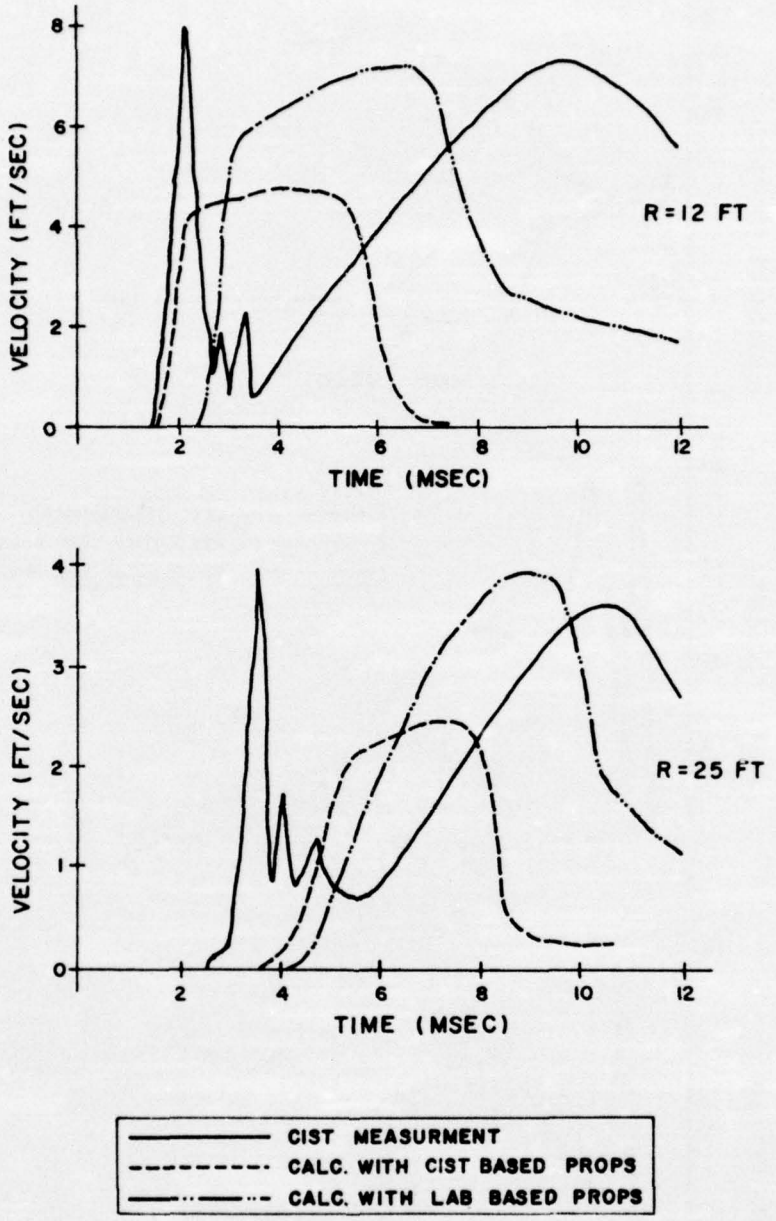

FIG. 28 HORIZONTAL - COMPARISON OF MEASURED AND CALCULATED CIST WAVEFORMS AT Z = 35 FT.

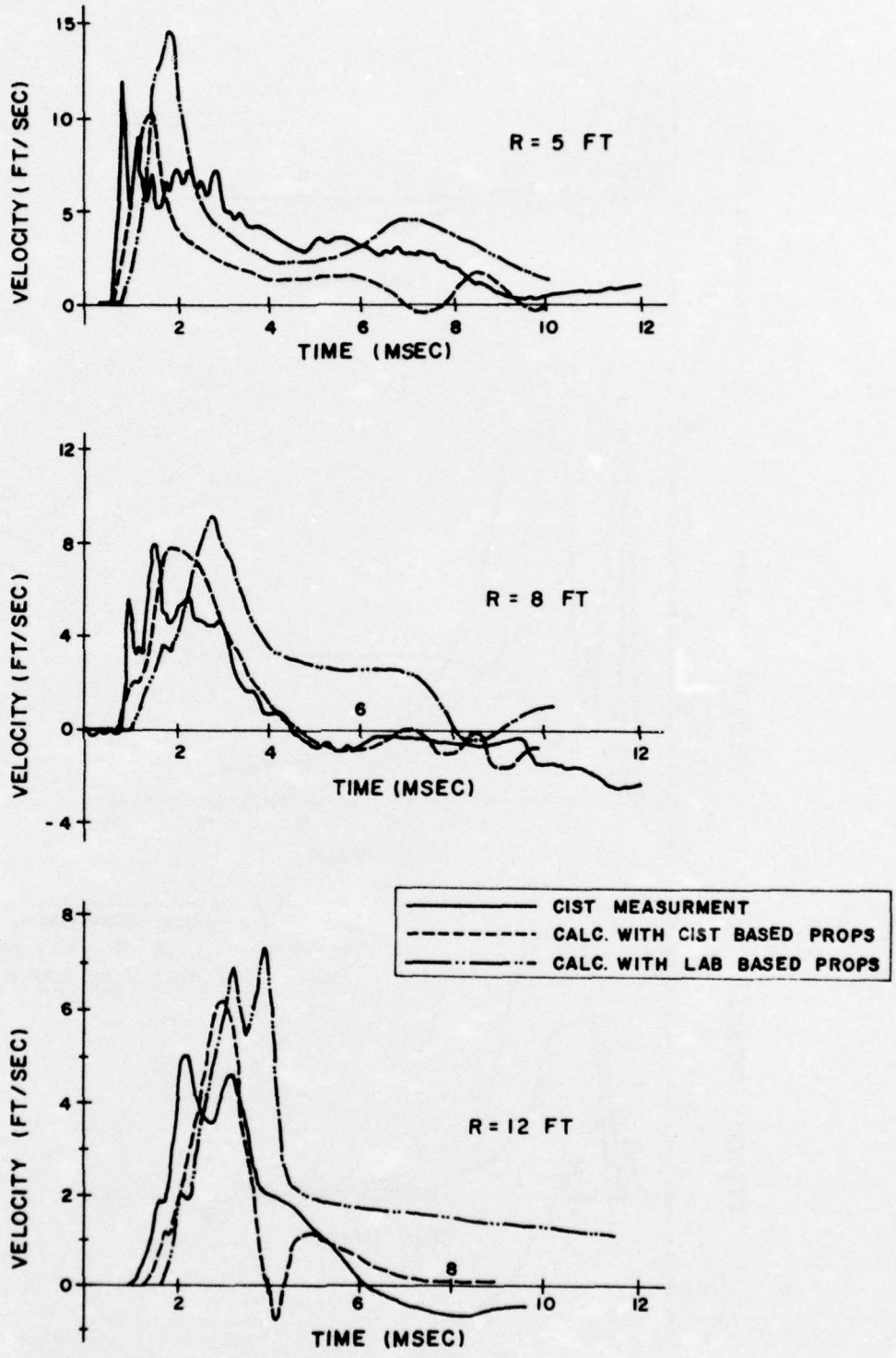

FIG. 29 HORIZONTAL- COMPARISON OF MEASURED AND CALCULATED CIST WAVEFORMS AT Z = 29.5 FT.

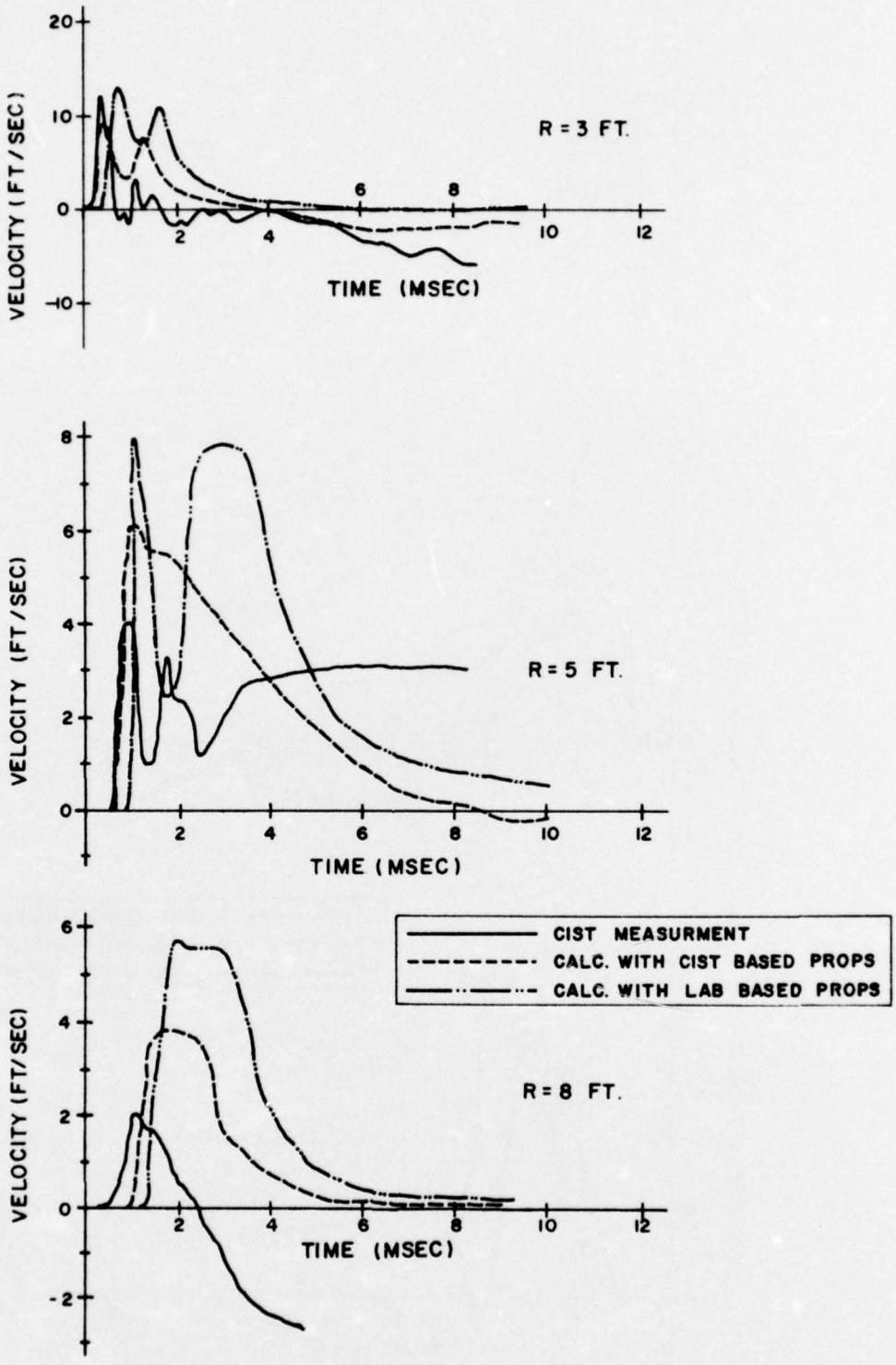

FIG. 30 HORIZONTAL - COMPARISON OF MEASURED AND CALCULATED CIST WAVEFORMS AT Z = 28.5 FT.

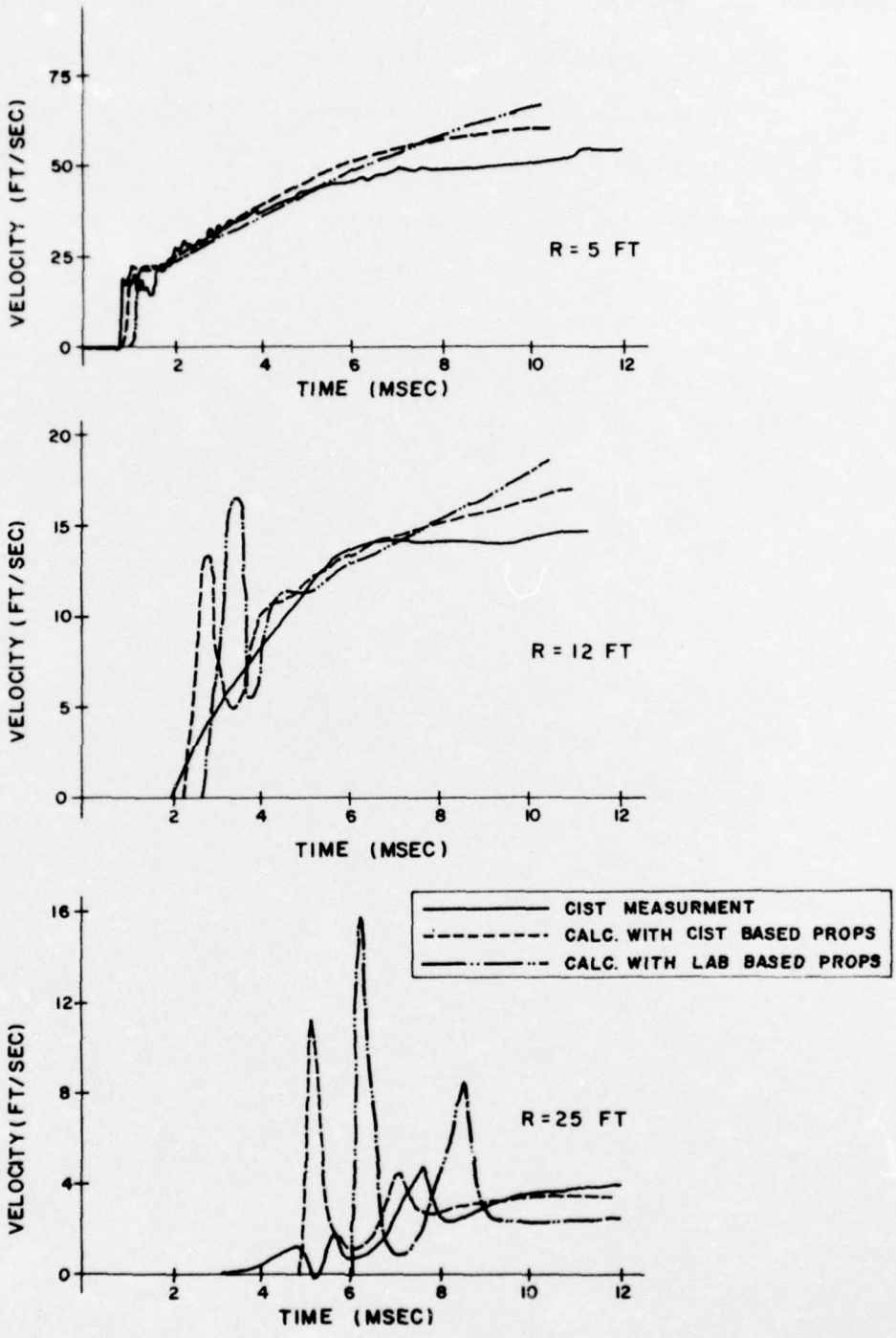

FIG. 31 HORIZONTAL - COMPARISON OF MEASURED AND CALCULATED CIST WAVEFORMS AT Z = 18 FT.

within the layers. Because most of the non-uniformities are always unknown and, even if known, certainly can not be included in two dimensional axisymmetric CIST computations, it seems futile to hope that they can ever be represented in a CIST computation of the type performed in this study.

VI CONCLUSIONS AND RECOMMENDATIONS

By means of an iteration procedure in which a cap model fitted to laboratory data was altered in such a way as to lead to improved results in the computation of CIST 12, a model has been obtained for the HARD PAN site which agrees reasonably well with both laboratory and in situ measurements. This model is now being used in a number of ground shock and structure-medium interaction computations for the HARD PAN SITE.

The construction of the final cap model (which is consistent with laboratory as well as CIST data) presented little difficulty in this study. It is not clear, however, whether this is a general phenomenon or whether it is merely a fortunate consequence of the behavior of the HARD PAN site in particular. Therefore, it is envisioned that a number of other sites at which CIST tests have been performed will be studied using the procedure developed in this investigation. These sites include the Nevada Test Site (CIST 5, 6, 7) the MIDDLE GUST wet site (CIST 9) and the DICE THROW site (CIST 15).

The present study has shown that the vertical velocities observed during a CIST test are too sensitive to layer irregularities to be useful for fitting models. For this reason, it is recommended that emphasis should be placed on fielding additional and/or redundant horizontal velocity gauges in future CIST tests. This will permit one to obtain estimates of data scatter and uncertainty, and to establish the magnitude of baseline shift which can be expected in the CIST measurements.

Such information would enable the modeler to judge better the adequacy of any particular fit and to evaluate the accuracy which can be achieved in a ground shock computation using the model.

Because the amount of useful data obtained from CIST is limited to horizontal motions and may not directly relate to deep outrunning, airblast or crater induced behavior, the need for additional information is clear. Especially when the site is anisotropic, tests which excite primarily vertical motions, e.g., DISK HEST or above ground bursts, are important so that laboratory data (which is obtained mainly from vertically cored samples) may be related to the in situ behavior in that direction. Hopefully, a comparison of laboratory and in situ behavior will become available for the CIST configuration when TERRA TEK, Inc., completes tests in which CIST-like stress paths will be applied to laboratory specimens and the results compared to CIST measurements and calculations.

As far as the HARD PAN site in particular is concerned, it is recommended that the material model obtained in this study be used in a calculation of the DISK HEST which was conducted as one of the events in the HARD PAN series. A better assessment of the current HARD PAN model may then be made and, if required, an improved model could be constructed to take into account this additional in situ information.

REFERENCES

[1] Sandler, I.S., Wright, J.P., and Baron, M.L., "Ground Motion Calculations for Events II and III of the MIDDLE GUST Series", DNA Report No. 3290T, Weidlinger Associates, 5 April 1974.

[2] Sandler, I.S., Wright, J.P., Baron, M.L., and Kovarna, J., "Ground Motion Calculations for the MIXED COMPANY Event of the MIDDLE NORTH Series", Contract Report S-74-4 for U.S. Army Waterways Experiment Station, Weidlinger Associates, October 1974.

[3] Bratton, J.L. and Port, R.J., "Material Models, Calculations and Experimental Results-MIDDLE GUST IV", DNA Long Range Planning Meeting Proceedings, June 1973.

[4] Davis, S.E., "General Test Plan for the Cylindrical In-Situ Test (CIST)", Report AFWL-TR-74-136, June 1974.

[5] DiMaggio, F.L., and Sandler I.S., "Material Model for Soils", J. Engrg. Mech., ASCE, June 1971, pp. 935-950.

[6] Sandler, I.S., DiMaggio, F.L. and Baladi, G.Y., "A Generalized Cap Model for Geological Materials", DNA Report No. 3443T, Weidlinger Associates, November 1974.

[7] Sandler, I.S. and Rubin D., "A Modular Subroutine for the Cap Model", DNA Report No. 3875F, Weidlinger Associates, January 1976.

[8] Ehrgott, J.W., "Preshot Calculational Properties for Project HARD PAN I, Event 2", U.S. Army Engineer Waterways Experiment Station, Soils and Pavements Laboratory, Vicksburg, Mississippi, 12 November 1974.

[9] Ehrgott, J.Q., "Preshot Free-Field Calculational Properties for Project HARD PAN I, Event 3", U.S. Army Engineer Waterways Experiment Station, Soils and Pavements Laboratory, Vicksburg, Mississippi, March 1975.

[10] Pinker, Capt., R.W. and Melzer, L.S., "Idealized Geologic Profile for Calculations for HARD PAN I, Event 1", AFWL/DEV Memorandum for the Record, Kirtland Air Force Base, New Mexico, 30 August 1974.

[11] Matthews, A.T. and Bleich H.H., "Dynamic Response of a Cylindrical Cavity of Finite Length in a Bilinear Material", DNA Report No. 3756T, Weidlinger Associates, June 1975.

APPENDIX

Brief Description of the LAYER Code

The LAYER code is an explicit two dimensional axisymmetric dynamic finite difference code designed for the efficient solution of problems involving wave propagation in a layered medium. The code can accept a wide range of material model behavior for each layer of a horizontally bedded geometry and can be modified to accept arbitrary initial conditions and traction and/or velocity boundary conditions. The use of reasonably "quiet" transmitting boundaries allows half-space problems to be efficiently solved. The code neglects material transport (convection)effects.

A typical grid layout for the LAYER code is shown in Fig. A-1. Each of the layers consists of a homogeneous single phase transversely isotropic material. Non-slip contact between layers is assumed, although slip and seperation effects can be modeled by introducing an additional thin layer of a material which is weak in shear and/or tension.

As can be seen from Fig. A-1, various types of boundary conditions may be applied. These include applied surface pressures as well as rigid, roller and "transmitting" boundaries. In addition, the annulus shown in Fig. A-1 may be replaced by a solid cylinder by setting $r_0 = 0$. This automatically introduces the proper symmetry and continuity boundary conditions along the center line. Plane strain problems may be

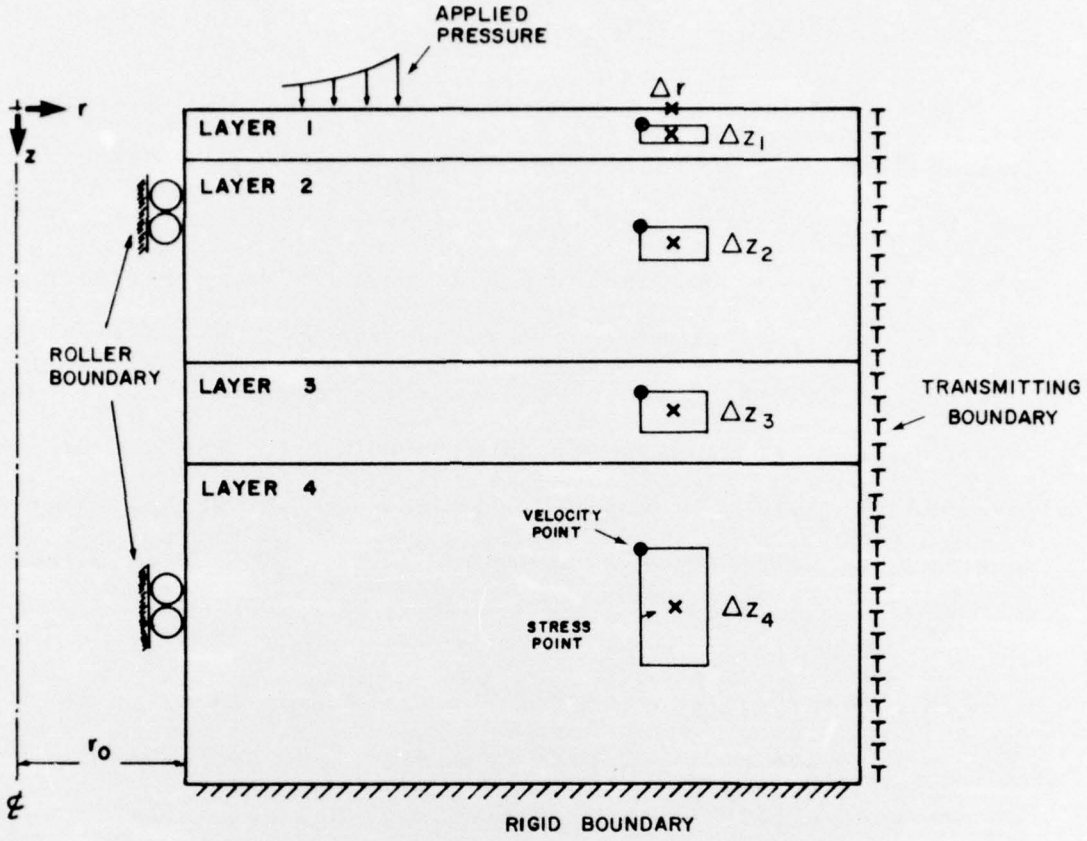

FIG. A-1 TYPICAL LAYER CODE GRID LAYOUT

solved by using a large value of r_0 .

Because transport, or convective, effects are ignored in LAYER, it is possible to formulate the governing continuum equations so that the stress and velocity are the only unknown field variables. At any point (r, z), let σ_r, σ_z, σ_θ and τ represent the radial, axial, tangential and shear stress components in the cylindrical (r, z) coordinate system as functions of r, z and time t and let u and v represent the radial and axial velocity components at (r, z, t). The governing equations consist of the equations of motion

$$\frac{\partial u}{\partial t} = \frac{1}{\rho}\left(\frac{\partial \sigma_r}{\partial r} + \frac{\sigma_r - \sigma_\theta}{r} + \frac{\partial \tau}{\partial z}\right)$$

$$\frac{\partial v}{\partial t} = \frac{1}{\rho}\left(\frac{\partial \sigma_z}{\partial z} + \frac{\partial \tau}{\partial r} + \frac{\tau}{r}\right) + g$$

in which ρ is the local density and g is the acceleration of gravity, together with the constitutive equations, which may be represented as

$$\frac{\partial \sigma_r}{\partial t} = M_{rr}\frac{\partial u}{\partial r} + M_{rz}\frac{\partial v}{\partial z} + M_{r\theta}\frac{u}{r}$$

$$\frac{\partial \sigma_z}{\partial t} = M_{zr}\frac{\partial u}{\partial r} + M_{zz}\frac{\partial v}{\partial z} + M_{z\theta}\frac{u}{r}$$

$$\frac{\partial \sigma_\theta}{\partial t} = M_{\theta r}\frac{\partial u}{\partial r} + M_{\theta z}\frac{\partial v}{\partial z} + M_{\theta\theta}\frac{u}{r}$$

$$\frac{\partial \tau}{\partial t} = M_{\tau\gamma}\left(\frac{\partial u}{\partial z} + \frac{\partial v}{\partial r}\right)/2$$

in which the moduli M_{ij} are defined by the local constitutive model.

The finite difference analog of the above equations is constructed for LAYER by using a staggered grid, Fig. (A-1), and by taking central differences for all spatial derivatives, forward time derivatives in the equations of motion, and backward time derivatives in the constitutive equations. Therefore, at any time, the equations of motion are first employed to determine the new velocity field and this field is then used to construct the strain rate components $\partial u/\partial r$, $\partial v/\partial z$, u/r and $(\partial u/\partial z + \partial v/\partial r)/2$. These are then used in the material subroutine to obtain the new stresses.

The LAYER computational grid is orthogonal with a constant radial mesh size, Δr, and a variable vertical mesh size, Δz, which changes arbitrarily with depth. Because long and narrow grid elements can sometimes introduce significant numerical errors into a computation, the aspect ratio, $\Delta r/\Delta z$, for each mesh point is generally kept between 1/5 and 5. Of course, the usual Courant, Friedrichs, Lewy stability condition governs the choice of time step, Δt.

There are several additional features of interest in LAYER. In order to improve efficiency in solving certain types of extended ground shock problems, LAYER has a restart capability as well as an option to shift the computational grid in space (dropping grid cells behind and acquiring undisturbed new cells in front). As far as output is concerned, quantities such as stress and velocity components, stress invariants, or other desired variables, are written at each time step and at

specified points of interest on a binary tape. Further, peak stresses, velocities, and displacements are stored for all depths at given ranges, and peak displacements are stored for all ranges at specified depths. Plots of the time histories and cross plots of pairs of quantities can easily be obtained.

The LAYER code has been implemented on a number of computers, but it has been used principally on Control Data Corporation equipment, specifically on CDC 6600 and 7600 machines. A large problem may have about 10,000 space points and involve about 2000 time steps. Such a run typically requires about three hours of central processor time on a CDC 6600 if the cap model is used.

DISTRIBUTION LIST

DEPARTMENT OF DEFENSE

Assistant to the Secretary of Defense
Atomic Energy
ATTN: Honorable Donald R. Cotter

Director
Defense Advanced Research Projects Agency
ATTN: NMRO
ATTN: PMO
ATTN: STO
ATTN: Tech. Lib.

Director
Defense Civil Preparedness Agency
ATTN: Admin. Officer

Defense Documentation Center
12 cy ATTN: TC

Director
Defense Intelligence Agency
ATTN: DI-7E
ATTN: DI-7D, Edward O' Farrell
ATTN: DT-1C

Director
Defense Nuclear Agency
ATTN: STSI, Archives
ATTN: DDST
2 cy ATTN: SPSS
3 cy ATTN: STTL, Tech. Lib.

Director of Defense Research & Engineering
ATTN: DD/TWP
ATTN: AD/SW
ATTN: DD/S&SS
ATTN: DD/I&SS

Commander
Field Command
Defense Nuclear Agency
ATTN: FCPR

Director
Interservice Nuclear Weapons School
ATTN: Tech. Lib.

Director
Joint Strat. Tgt. Planning Staff, JCS
ATTN: STINFO, Library

Chief
Livermore Division, Field Command, DNA
ATTN: FCPRL

DEPARTMENT OF THE ARMY

Director
BMD Advanced Tech. Ctr.
ATTN: CRDABH-S
ATTN: CRDABH-X

Dep. Chief of Staff for Rsch., Dev. & Acq.
ATTN: Tech. Lib.

DEPARTMENT OF THE ARMY (Continued)

Chief of Engineers
Department of the Army
ATTN: DAEN-MCE-D
ATTN: DAEN-RDM

Deputy Chief of Staff for Ops. & Plans
ATTN: Tech. Lib.

Commander
Harry Diamond Laboratories
ATTN: DRXDO-TI, Tech. Lib.
ATTN: DRXDO-NP

Commander
Redstone Scientific Information Ctr.
ATTN: Chief, Documents

Director
U.S. Army Ballistic Research Labs.
ATTN: J. H. Keefer
ATTN: W. Taylor
ATTN: Tech. Lib., Edward Baicy
ATTN: DRXBR-X, Julius J. Meszaros

Commander
U.S. Army Engineer Center
ATTN: ATSEN-SY-L

Division Engineer
U.S. Army Engineer Div., Huntsville
ATTN: HNDSE-R, Michael M. Dembo

Division Engineer
U.S. Army Engineer Div., Ohio River
ATTN: Tech. Lib.

Director
U.S. Army Engr. Waterways Exper. Sta.
ATTN: Guy Jackson
ATTN: William Flathau
ATTN: John N. Strange
ATTN: Leo Ingram
ATTN: Tech. Lib.

Commander
U.S. Army Mat. & Mechanics Rsch. Ctr.
ATTN: Tech. Lib.

Commander
U.S. Army Materiel Dev. & Readiness Cmd.
ATTN: Tech. Lib.

Commander
U.S. Army Nuclear Agency
ATTN: Tech. Lib.

DEPARTMENT OF THE NAVY

Chief of Naval Material
ATTN: MAT 0323

Chief of Naval Operations
ATTN: OP-985F
ATTN: OP-03EG

DEPARTMENT OF THE NAVY (Continued)

Chief of Naval Research
ATTN: Tech. Lib.
ATTN: Code 464, Jacob L. Warner
ATTN: Code 464, Thomas P. Quinn
ATTN: Nicholas Perrone

Officer-in-Charge
Civil Engineering Laboratory
ATTN: Stan Takahashi
ATTN: Tech. Lib.

Commander
Naval Electronic Systems Command
ATTN: PME 117-21A

Commander
Naval Facilities Engineering Command
ATTN: Code 04B
ATTN: Tech. Lib.
ATTN: Code 03A

Superintendent (Code 1424)
Naval Postgraduate School
ATTN: Code 2124, Tech. Rpts. Librarian

Director
Naval Research Laboratory
ATTN: Code 2027, Tech. Lib.

Commander
Naval Sea Systems Command
ATTN: ORD-91313, Lib.

Commander
Naval Ship Engineering Center
ATTN: Tech. Lib.

Commander
Naval Ship Rsch & Development Ctr.
ATTN: Code L42-3, Library

Commander
Naval Ship Rsch & Development Ctr.
Underwater Explosive Research Division
ATTN: Tech. Lib.

Commander
Naval Surface Weapons Center
ATTN: Code WX-21, Tech. Lib.
ATTN: Code WA-501, Navy Nuc. Prgms. Off.

Commander
Naval Surface Weapons Center
ATTN: Tech. Lib.

President
Naval War College
ATTN: Tech. Lib.

Commanding Officer
Naval Weapons Evaluation Facility
ATTN: Tech. Lib.

Director
Strategic Systems Project Office
ATTN: NSP-43, Tech. Lib.

DEPARTMENT OF THE AIR FORCE

AF Geophysics Laboratory, AFSC
ATTN: SUOL, AFCRL, Rsch. Lib.

AF Institute of Technology, AU
ATTN: Library, AFIT, Bldg. 640, Area B

AF Weapons Laboratory, AFSC
ATTN: DEV, Jimmie L. Bratton
ATTN: DES, M. A. Plamondon
ATTN: Robert Port
ATTN: DYT
ATTN: Robert Henny
ATTN: SUL

Headquarters
Air Force Systems Command
ATTN: DLCAW
ATTN: Tech. Lib.

Commander
Foreign Technology Division, AFSC
ATTN: TD-BTA, Library

HQ USAF/IN
ATTN: INATA

HQ USAF/PR
ATTN: PRE

HQ USAF/RD
ATTN: RDQPN

Commander
Rome Air Development Center, AFSC
ATTN: EMTLD, Doc. Lib.

SAMSO/MN
ATTN: MMH

Commander in Chief
Strategic Air Command
ATTN: NRI-STINFO, Library

ENERGY RESEARCH & DEVELOPMENT ADMINISTRATION

University of California
Lawrence Livermore Laboratory
ATTN: Tech. Info., Dept. L-3

Los Alamos Scientific Laboratory
ATTN: Doc. Con. for Reports Lib.
ATTN: Doc. Con. for G. R. Spillman
ATTN: Doc. Con. for R. J. Bridwell

Sandia Laboratories
Livermore Laboratory
ATTN: Doc. Con. for Tech. Lib.

Sandia Laboratories
ATTN: Doc. Con. for 3141, Sandia Rpt. Coll.

U.S. Energy Rsch. & Dev. Admin.
Albuquerque Operations Office
ATTN: Doc. Con. for Tech. Lib.

U.S. Energy Rsch. & Dev. Admin.
Division of Headquarters Services
ATTN: Doc. Con. for Class. Tech. Lib.

ENERGY RESEARCH & DEVELOPMENT ADMINISTRATION (Continued)

U.S. Energy Rsch. & Dev. Admin.
Nevada Operations Office
ATTN: Doc. Con. for Tech. Lib.

Union Carbide Corporation
Holifield National Laboratory
ATTN: Civil Def. Res. Proj.
ATTN: Doc. Con. for Tech. Lib.

OTHER GOVERNMENT AGENCIES

Department of the Interior
Bureau of Mines
ATTN: Tech. Lib.

Department of the Interior
U.S. Geological Survey
ATTN: J. H. Healy
ATTN: Cecil B. Raleigh

DEPARTMENT OF DEFENSE CONTRACTORS

Aerospace Corporation
ATTN: Tech. Info. Services

Agbabian Associates
ATTN: M. Agbabian

Applied Theory, Inc.
2 cy ATTN: John G. Trulio

Avco Research & Systems Group
ATTN: Research Library, A-830, Rm. 7201

Battelle Memorial Institute
ATTN: Tech. Lib.

The BDM Corporation
ATTN: Tech. Lib.

The Boeing Company
ATTN: R. M. Schmidt
ATTN: Aerospace Library

California Research & Technology, Inc.
ATTN: Tech. Lib.
ATTN: Sheldon Shuster
ATTN: Ken Kreyenhagen

Calspan Corporation
ATTN: Tech. Lib.

Civil/Nuclear Systems Corp.
ATTN: Robert Crawford

University of Dayton
Industrial Security Super KL-505
ATTN: Hallock F. Swift

University of Denver
Colorado Seminary
ATTN: Sec. Officer for J. Wisotski
ATTN: Sec. Officer for Tech. Lib.

EG&G, Inc.
Albuquerque Division
ATTN: Tech. Lib.

DEPARTMENT OF DEFENSE CONTRACTORS (Continued)

General American Transportation Corp.
General American Research Division
ATTN: G. L. Neidhardt

General Electric Company
TEMPO-Center for Advanced Studies
ATTN: DASIAC

IIT Research Institute
ATTN: Tech. Lib.

Institute for Defense Analyses
ATTN: IDA, Librarian, Ruth S. Smith

Kaman AviDyne
Division of Kaman Sciences Corp.
ATTN: Tech. Lib.
ATTN: E. S. Criscione

Kaman Sciences Corporation
ATTN: Library

Lockheed Missiles & Space Co., Inc.
ATTN: Tech. Lib.

Lockheed Missiles & Space Company
ATTN: Tech. Info. Ctr., D/Coll
ATTN: Tom Geers, Dept. 52-33, Bldg. 205

McDonnell Douglas Corporation
ATTN: Robert W. Halprin

Merritt Cases, Incorporated
ATTN: J. L. Merritt
ATTN: Tech. Lib.

The Mitre Corporation
ATTN: Library

Nathan M. Newmark
Consulting Engineering Services
ATTN: Nathan M. Newmark

Physics International Company
ATTN: Doc. Con. for Tech. Lib.
ATTN: Doc. Con. for Larry A. Behrmann
ATTN: Doc. Con. for Fred M. Sauer
ATTN: Doc. Con. for E. T. Moore
ATTN: Doc. Con. for Robert Swift
ATTN: Doc. Con. for Charles Godfrey
ATTN: Doc. Con. for Dennis Orphal

R & D Associates
ATTN: Tech. Lib.
ATTN: Harold L. Brode
ATTN: Cyrus P. Knowles
ATTN: Bruce Hartenbaum
ATTN: Albert L. Latter
ATTN: Henry Cooper
ATTN: J. G. Lewis
ATTN: William B. Wright, Jr.
ATTN: Jerry Carpenter

Science Applications, Inc.
ATTN: D. E. Maxwell
ATTN: David Bernstein

Science Applications, Inc.
ATTN: Michael McKay
ATTN: Tech. Lib.

DEPARTMENT OF DEFENSE CONTRACTORS (Continued)

Science Applications, Inc.
ATTN: R. A. Shunk

Southwest Research Institute
ATTN: Wilfred E. Baker
ATTN: A. B. Wenzel

Stanford Research Institute
ATTN: George R. Abrahamson
ATTN: Carl Peterson
ATTN: Burt R. Gasten

Systems, Science & Software, Inc.
ATTN: Tech. Lib.
ATTN: Ted Cherry
ATTN: Thomas D. Riney
ATTN: Donald R. Grine

Terra Tek, Inc.
ATTN: Tech. Lib.
ATTN: Sidney Green

Tetra Tech, Inc.
ATTN: Tech. Lib.
ATTN: Li-San Hwang

TRW Systems Group
ATTN: D. H. Baer, R1-2136
ATTN: I. E. Alber, R1-1008
ATTN: Tech. Info. Ctr., S-1930
ATTN: R. K. Plebuch, R1-2078
2 cy ATTN: Peter K. Dai, R1-2170

TRW Systems Group
San Bernardino Operations
ATTN: E. Y. Wong, 527/712

DEPARTMENT OF DEFENSE CONTRACTORS (Continued)

Universal Analytics, Inc.
ATTN: E. I. Field

URS Research Company
ATTN: Tech. Lib.

The Eric H. Wang Civil Engineering Rsch. Fac.
ATTN: Neal Baum
ATTN: Larry Bickle

Washington State University
Administrative Office
ATTN: Arthur Miles Hohorf for George Duval

Weidlinger Assoc. Consulting Engineers
ATTN: Melvin L. Baron
ATTN: J. W. Wright
ATTN: Dr. I. S. Sandler

Weidlinger Assoc. Consulting Engineers
ATTN: J. Isenberg

Westinghouse Electric Company
Marine Division
ATTN: W. A. Volz